AD-A050 049 HONEYWELL CORPORATE MATERIAL SCIENCES CENTER BLOOMIN--ETC F/G 20/5
AN INVESTIGATION OF LASER INTERACTIONS.(U)
NOV 77 J F READY

UNCLASSIFIED F44620-73-C-0022
AFOSR-TR-78-0070 NL

1 OF 1
AD A050049

END
DATE FILMED
3-78
DDC

(18) (19) AFOSR-TR-78-0070

(2)

(6) AN INVESTIGATION OF LASER INTERACTIONS.

Final Report on Contract (15) F44620-73-C-0022

Covering Period from

(9) Final rept. 15 Dec 1972 to 30 Sep 1977,

by

(10) John F. Ready

5/4 Honeywell Corporate Material Sciences Center
10701 Lyndale Avenue South
Bloomington, Minnesota 55420

(16) 2301
(17) A4

to

Air Force Office of Scientific Research
Directorate of Physics
Bolling Air Force Base, Bldg. 410
Washington, D.C. 20332

(11) Nov 1977
(12) 68 P.

Approved for Public Release; Distribution Unlimited

UNCLASSIFIED

SECURITY CLASSIFICATION OF THIS PAGE (When Data Entered)

REPORT DOCUMENTATION PAGE		READ INSTRUCTIONS BEFORE COMPLETING FORM
1. REPORT NUMBER AFOSR-TR- 78-0070	2. GOVT ACCESSION NO.	3. RECIPIENT'S CATALOG NUMBER
4. TITLE (and Subtitle) AN INVESTIGATION OF LASER INTERACTIONS		5. TYPE OF REPORT & PERIOD COVERED Final Dec. 15, 1972-Sept. 30, 1977
		6. PERFORMING ORG. REPORT NUMBER
7. AUTHOR(s) John F. Ready		8. CONTRACT OR GRANT NUMBER(s) F44620-73-C-0022
9. PERFORMING ORGANIZATION NAME AND ADDRESS Honeywell Corporate Material Sciences Center 10701 Lyndale Avenue South Bloomington, Minnesota 55420		10. PROGRAM ELEMENT, PROJECT, TASK AREA & WORK UNIT NUMBERS 2301-A4 61102F
11. CONTROLLING OFFICE NAME AND ADDRESS Air Force Office of Scientific Research/NP Directorate of Physics Bolling Air Force Base, Bldg. 410, Wash.D.C. 20332		12. REPORT DATE November, 1977
		13. NUMBER OF PAGES 67
14. MONITORING AGENCY NAME & ADDRESS (if different from Controlling Office)		15. SECURITY CLASS. (of this report) UNCLASSIFIED
		15a. DECLASSIFICATION/DOWNGRADING SCHEDULE

16. DISTRIBUTION STATEMENT (of this Report)

Approved for Public Release; Distribution Unlimited

17. DISTRIBUTION STATEMENT (of the abstract entered in Block 20, if different from Report)

18. SUPPLEMENTARY NOTES

19. KEY WORDS (Continue on reverse side if necessary and identify by block number)

Lasers	Laser Interaction with Materials
Material Damage	Reflectivity
TEA Lasers	Plexiglass
Potassium Chloride	Silicone
	Epoxy

1000 Mw/69 cm

20. ABSTRACT (Continue on reverse side if necessary and identify by block number)

This report describes work performed in a continuous program of investigations on the mechanisms by which high power pulsed CO_2 laser radiation interacts with target surfaces. The experimental work has been performed using a pulsed CO_2 TEA laser capable of delivering up to 10^9 w/cm^2 to the target surface in a pulse of duration around 100 nanoseconds. Results described in this report include the following; →

UNCLASSIFIED

SECURITY CLASSIFICATION OF THIS PAGE(When Data Entered)

Abstract, continued

The diffuse reflectivity of steel and titanium targets has been measured under varying conditions of TEA irradiation.

The shock pressure coupled into metallic and potassium chloride targets by the laser-supported absorption wave has been measured interferometrically, and the results compared to catastrophic material failure in potassium chloride.

The mass removal from plastic targets has been determined for various parameters of laser irradiation.

TABLE OF CONTENTS

LIST OF ILLUSTRATIONS

SECTION I
INTRODUCTION

This report describes work performed in a continuing program of investigations of the interaction of high power pulsed CO_2 laser radiation with target materials. This program has extended over a period of almost five years, from 15 December 1972 until 30 September 1977. At the time that the work began in 1972, there were several important unresolved issues in the physics of the interaction of high power CO_2 laser radiation with materials. These issues included: The mechanism of the initiation and growth of the laser-supported absorption wave, the effect of the laser-supported absorption wave in shielding the target from incident laser radiation, coupling of both thermal energy and impulse to the target, the effect of the irradiation on optical properties of the target and the effect of repeated pulses on the same target area. Many of these issues have been resolved satisfactorily, as a result of work performed under this contract and of work performed at other laboratories. The coupling of long wavelength infrared laser energy into materials is much better understood than in 1972. Descriptions of the physics of the interaction are now available.

In the work performed under this contract, we developed quantitative data on the interaction of the high power CO_2 laser beams in a regime of laser parameters which had not been well explored previously.

For this work we used a pulsed CO_2 TEA laser operating at a wavelength of 10.6μm. This laser emits pulses with peak power up to 10 megawatts and can be focussed to deliver power densities at the target in the range of 10^8 to $10^9 w/cm^2$. The pulse shape can be varied by changing the gas mixture in the laser. The gas mixture consists of CO_2, N_2 and He. When the mixture is deficient in N_2, the laser output consists of a single spike of half-width 100 nanoseconds. When N_2 is added to the gas mixture, a longer lower power tail of duration several microseconds is present, in addition to the initial shorter spike. The initial spike is unchanged in amplitude and duration, but the addition of the longer tail increases the total energy by a factor around 3. In this report we shall characterize measurements as being made with N_2 off or N_2 on in the laser to describe these two different pulse shapes.

The work called for under this contract involved several specific areas of measurement, including measurement of impulse delivered to the target, measurement of pressure generated in the target, measurement of ion energy and species in the blowoff material, measurement of the change of specular reflectivity during the laser pulse, and measurement of the diffuse reflectivity. Work carried on in

earlier portions of this program has been described in previous interim reports[1,2,3,4]. Some portions of the work have been completely described in these reports. In order to make the present report self-contained and to show the relationship of the work performed in the last year to previous work, we shall briefly describe some of the previous measurements which have been reported previously.

· Measurement of impulse delivered to target materials by the CO_2 laser pulse. This portion of the work used a linear velocity transducer to measure the motion of the entire target when it was struck by the laser pulse. The target was mounted on a magnetic rod in the linear velocity transducer. The motion of the entire structure induced a voltage in the pickup coil of the transducer. The voltage provided a direct measurement of the velocity of the structure and hence of the impulse. Measurements were obtained as a function of target material, ambient air pressure, target diameter and laser power density. The impulse decreased with decreasing ambient air pressure down to around 10 torr. For air pressures below 10 torr, a small residual component of impulse was still present, because of target recoil from vaporized material. This value is approximately 0.4 dyne-second. At one atmosphere pressure, the quantitative value of the impulse is approximately 5 to 10 dyne-second.

These results may be understood in terms of a model in which kindling of the laser-supported absorption wave above the surface is responsible for the observed impulse. The laser-supported absorption wave is intercepted only partly by targets of small diameter, so that the total impulse transferred to a given target also increases as a function of the target diameter.

These results have been described completely in a previous report[2] and in a published paper[5].

· Measurement of the specular reflectivity of the target surface as a function of time during irradiation. These measurements were carried out using a probe beam from a continuous laser. The probe beam is focussed on the same area struck by the TEA laser beam. The temporal variation of light specularly reflected from the area struck by the TEA laser pulse yields the time-resolved specular reflectivity. The temporal variation of the specular reflectivity was measured as the function of ambient air pressure, probe laser wavelength, TEA laser power density, pulse shape, and accumulated number of pulses on the same area. Measurements as a function of ambient air pressure indicate that the change due to a single laser shot is smaller at higher values of the ambient air pressure, indicating the effect of the laser-supported absorption wave in shielding the target surface. At low values of ambient

air pressure, less than or equal to 10 torr, the laser-supported absorption wave has diminished. Under these conditions of reduced ambient air pressure, the change in specularly reflectivity is much enhanced. Results at two different probing laser wavelengths of 9.6μm and 0.6328μm indicate a much greater effect at the shorter wavelength, and show that the dominant effect is etching and roughening of the surface on a scale of a few micrometers. Effects are greater for target materials with relatively low initial reflectivity, for example steel, as compared to materials with higher initial reflectivity, such as aluminum.

Quantitative descriptions of these results have been presented completely in previous reports[2,3] and in a published paper[6].

· A time-of-flight spectrometer to measure the ion energy spectrum in the blowoff material. We have developed a unique method of data reduction to obtain the time-resolved, mass-resolved and energy-resolved spectrum of ions in the blowoff material produced in vacuum. We have presented data[3] for the development of the energy spectrum of ions emitted from the targets. The energy spectrum develops from relatively low energies early in the pulse to a higher energy near the end of the pulse. This indicates a transition from thermal energy to a directed energy of expansion of the material away from the target surface. It also indicates absorption of incoming laser energy in the blowoff material after it has been removed from the target surface. This is the dominant mechanism of heating the blowoff material and producing the observed energy spectra. Quantitative data on the total energy content of the blowoff material indicate that several percent of the incident laser energy can be removed by the blowoff material in its observed state of energy and ionization.

These results have been described completely in previous reports[2,3,4], and also in a paper which is being prepared for publication.

The body of this report will describe measurements carried out during the contract period from 15 December, 1976 through 30 September, 1977. These measurements include the following items:

· Measurement of the diffuse reflectivity of target surfaces irradiated under various conditions by the TEA laser.

· Measurements of pressure pulses coupled into the target materials and their correlation with damage in laser window materials. This was described partially in previous reports[3,4] but measurements have continued into the present contract period.

· Measurements of mass removal and hole depth for plastic materials supplied by the Air Force Materials Lab, as a function of laser power density, laser focussing conditions and pulse repetition rate.

SECTION II
BIBLIOGRAPHY OF PUBLICATIONS

The work performed under this contract has led to the following publications:

Impulse Produced by the Interaction of CO_2 TEA Laser Pulses, J. F. Ready, Applied Physics Letters, Vol. 25, No. 10, pp. 558-560, 15 November 1974.

Change of Reflectivity of Metallic Surfaces during Irradiation by CO_2-TEA Laser Pulses, J. F. Ready, IEEE Journal of Quantum Electronics, Vol. QE-12, No. 2, pp. 137-142, February, 1976.

Laser-Produced Shocks and their Relation to Material Damage, J. F. Ready, IEEE Journal of Quantum Electronics, to appear in February, 1978 issue.

Coupling of CO_2 Laser Energy into Ionized Blowoff Material, J. F. Ready, Optics Letters, to appear in 1978.

In addition, a paper entitled Ion Energy Spectra Produced in CO_2-TEA Laser Interactions is being prepared for submission to the Journal of Applied Physics.

Also, the following talks were presented at major scientific meetings:

Change of Reflectivity of Metallic Surfaces during Irradiation by CO_2-TEA Laser Pulses, J. F. Ready, presented at the 1975 IEEE/OSA Conference on Laser Engineering and Applications, May 28-30, 1975, Washington, D.C., abstract published in IEEE Journal of Quantum Electronics, p. 490, September, 1975.

Interaction of High Intensity Laser Radiation with Solid Surfaces, J. F. Ready, presented at the meeting of The Electrochemical Society, October 5-9, 1975, Dallas, Texas.

Laser-Produced Shocks and their Relation to Material Damage, J. F. Ready, presented at the 1977 IEEE/OSA Conference on Laser Engineering and Applications, June 1-3, 1977, Washington, D.C., abstract published in IEEE J. Quantum Electronics, p. 30, September, 1977.

Finally, talks reviewing work performed under this contract were presented to personnel at the Air Force Weapons Laboratory, Albuquerque, N.M., on June 25, 1973, again at the Air Force Weapons Laboratory on September 29, 1975, and at the Air Force Materials Laboratory, Wright-Patterson AFB, Ohio, on April 7, 1976.

SECTION III
REFLECTIVITY MEASUREMENTS

Our previous results involving measurement of time-resolved specular reflectivity had led us to a simple method for extending the measurements to include diffuse reflectivity. We had noted previously[2,6] that independent non-time-resolved measurements of specular reflectivity, diffuse reflectivity and absorptivity after the end of the laser pulse added to unity. These are measurements carried out by different techniques. This fact, of course, is true throughout the pulse but the conclusion is that our separate measuring techniques have sufficient reliability and reproducibility to measure two of the three parameters and to derive the third by subtraction.

Accordingly, we set up instrumentation to measure the diffuse reflectivity. This involved using an integrating ellipsoidal mirror. The measurement technique is similar to that used earlier for specular reflectivity. The ellipsoidal mirror collected all the probing light reflected from the target and thus allowed measurements of diffuse reflectivity.

In this experiment the target and the detector are placed at the two foci of the ellipsoid. As is well known, a light ray passing through one focus of the ellipsoid will reach the other focus, regardless of direction of travel. Thus the profile of the probe beam on the target is reimaged on the detector. The diffusely scattered probe radiation reaches the detector, regardless of the direction at which it leaves the target surface. Thus diffusely reflected radiation can be collected and measured with a high frequency detector. The ellipsoidal mirror has the advantage over a hemispherical mirror of reduced image size and conveniently large spatial separation between the two foci. Separation of components is important for accomodating suitable mounts for the target and the detector at the two foci.

In our measurements, we measured the diffusely reflected probe laser radiation separately by inserting a small opaque beam stop at the position on the ellipsoid struck by the specularly reflected beam. This allowed us to obtain the diffuse reflectivity spearately.

The ellipsoid is cast of aluminum-filled epoxy and has a coating of vacuum deposited aluminum. The major and minor axes are 24.85 and 23.85 centimeters respectively. The separation between the foci is 7 centimeters. This allows adequate room for mounting the target and the detector.

The two laser beams enter the ellipsoid through a hole in the mirror wall.

Losses can be expected from light being reflected out of the entrance hole and from absorption when the light is reflected from the mirror surface. Calibration is needed to establish the magnitude of flux loss. The calibration is carried out using a standard reflection target at one focus when the detector is at the other focus. The standard reflection target was manganese oxide for a visible probe laser beam.

Calibration of the total reflectivity at 10μm was accomplished by separate measurements on the damage spots after the irradiation. The measurements were performed using an integrating sphere reflectometer. They yield total reflectivity (specular plus diffuse reflectivity) at 10μm. Results are presented in Table V-1 for several targets and conditions of irradiation. For heavily damaged surfaces struck by several thousand consecutive pulses, the specular reflectivity has decreased to near 0^2. Thus we can equate the total reflectivity measured with the integrating sphere reflectometer to the diffuse reflectivity, and thus calibrate the integrating ellipsoid.

In order to be able to carry out measurements in vacuum, a bell jar vacuum station was constructed. The bell jar completely contains the ellipsoid, target and detector. The target mount allows remote movement of the target through a vacuum bellows assembly, so that fresh areas on the target can be presented for successive laser shots. The targets measured were stainless steel (300 series) and titanium.

The maximum laser power density that could be employed in this series of measurements was approximately $3 \times 10^7 w/cm^2$ delivered to the target. This value is lower than that employed in the previous measurements on specular reflectivity[2], because the beam had to be focussed with a longer focal length lens to deliver it through the hole in the ellipsoid to the position of the target. This meant that the minimum focal spot size on the target was larger and the laser power density was lower. Therefore the amount of damage that could be produced in a single shot was limited. As Table III-1 shows, irradiation of the titanium target with a single pulse of power 2.3×10^7 w/cm^2 did not produce a detectable change in total reflectivity at 10μm.

However after accumulating a number of shots on an area, the reflectivity was observed to change. We monitored the change in reflectivity with accumulated number of shots. Data are presented in Figures III-1 through III-4 for the change in reflectivity at 0.5145 micrometers when a argon laser was used as the probe beam.

Figure III-1 shows the diffuse reflectivity as a function of number of shots for a stainless steel target irradiated in vacuum (0.1 torr) at a power density of

TABLE III-1

Values of Total Reflectivity

Target	Shots	Conditions	Total Reflectivity 0.5μm	10μm
Steel	Initial Value	---	0.653	0.975
Steel	1	Vacuum, 2.3×10^7 w/cm^2	0.491	0.955
Steel	5835	Air, 2.3×10^7 w/cm^2	0.521	0.720
Titanium	Initial Value	---	0.504	0.986
Titanium	1	Air, 2.3×10^7 w/cm^2	0.508	0.986
Titanium	130	Air, 3.2×10^7 w/cm^2	0.352	0.918
Titanium	6780	Air, 2.3×10^7 w/cm^2	0.531	0.687

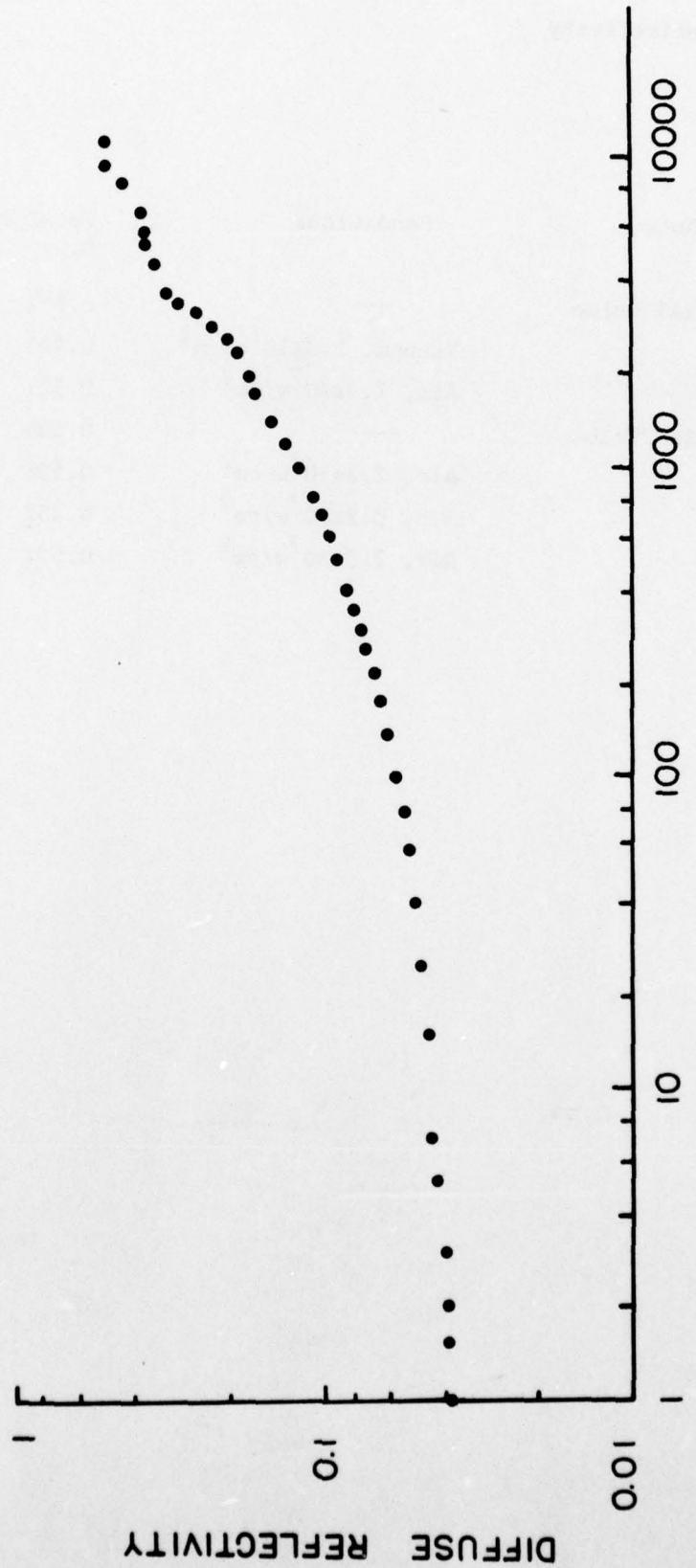

Figure III-1. Diffuse reflectivity at 0.5145μm for a stainless steel target irradiated in vacuum at a power density of $2.3 \times 10^7 w/cm^2$, as a function of number of shots.

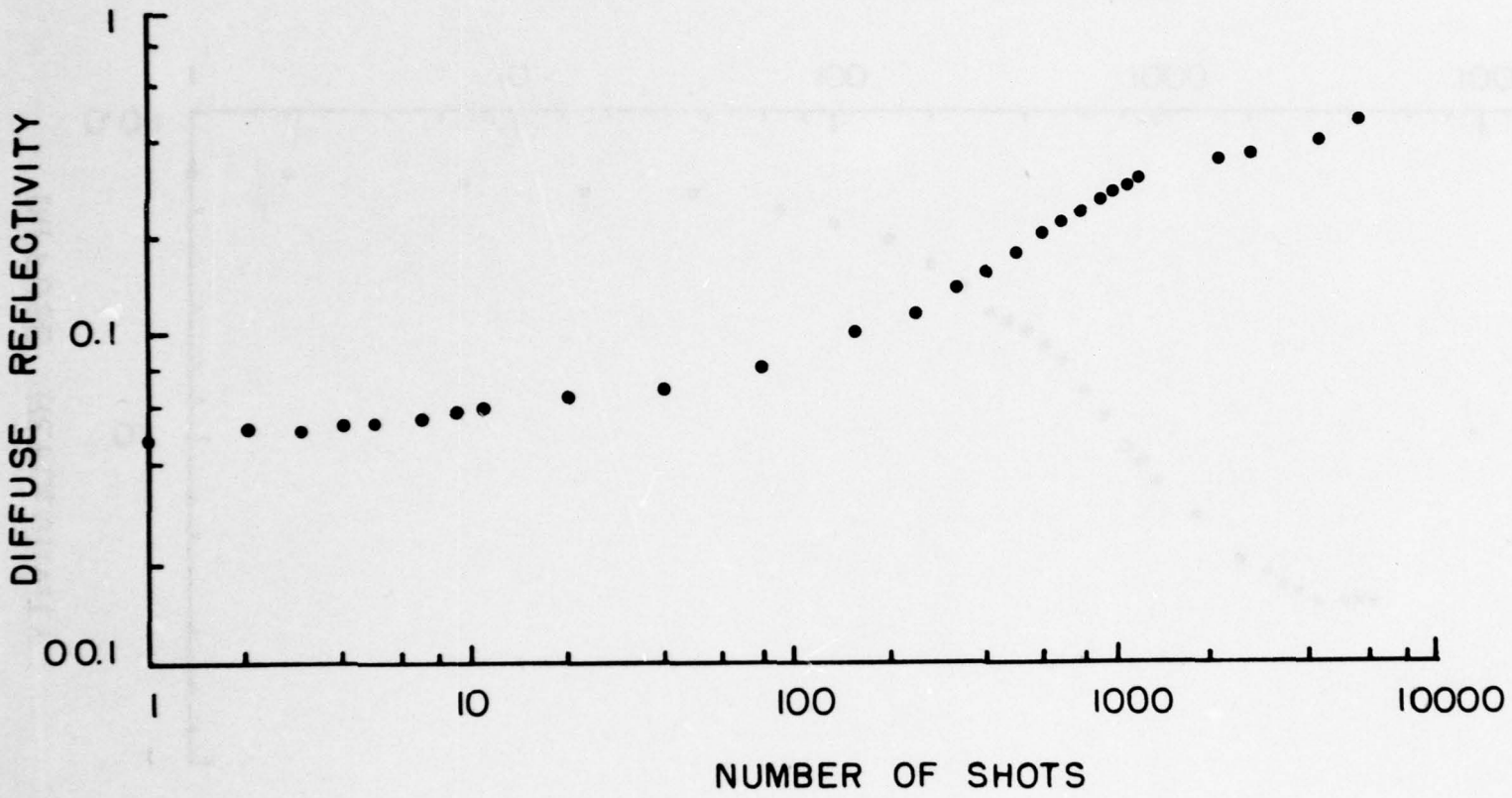

Figure III-2. Diffuse reflectivity at 0.5145μm for a stainless steel target irradiated in ambient air at a power density of $2.3 \times 10^7 w/cm^2$, as a function of number of shots.

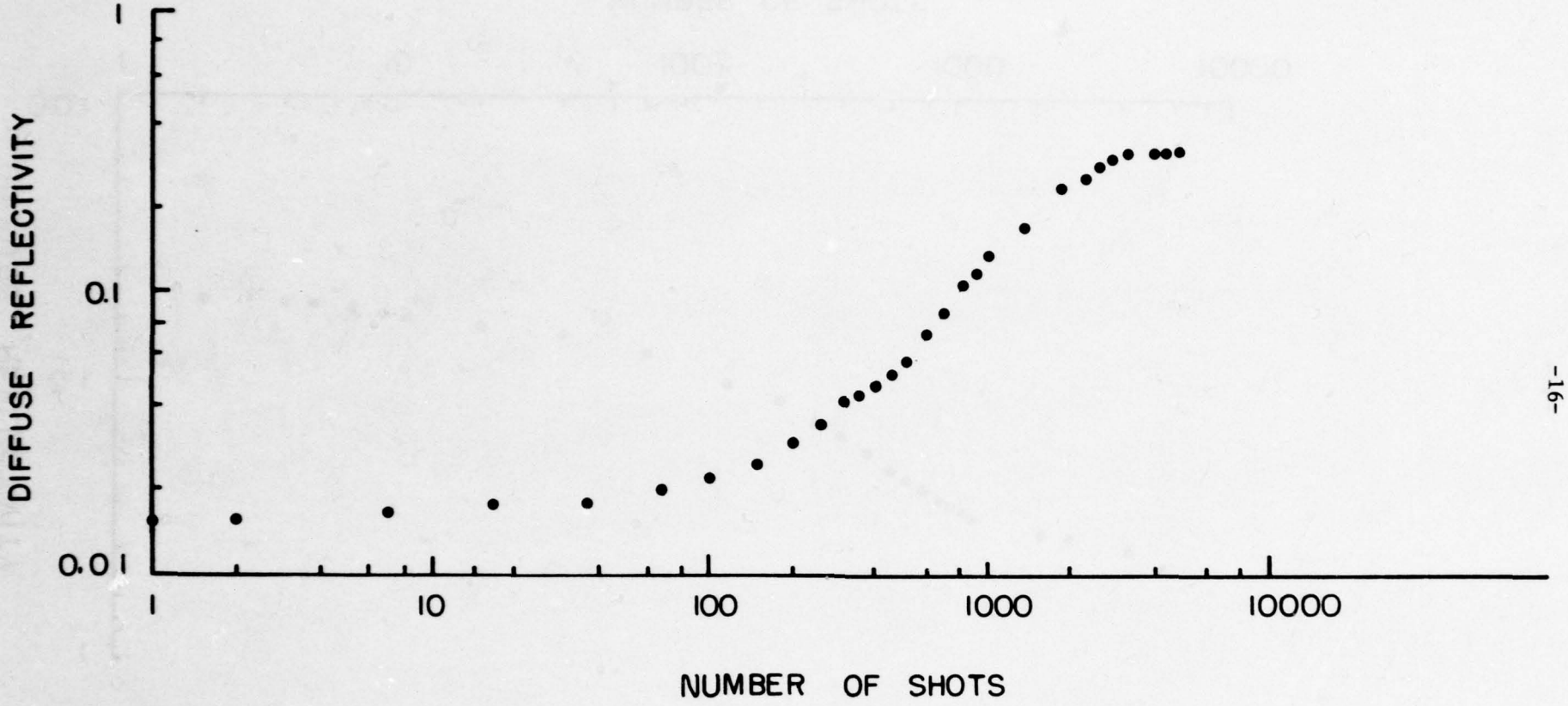

Figure III-3. Diffuse reflectivity at 0.5145μm for a titanium target irradiated in vacuum at a power density of $2.3 \times 10^7 w/cm^2$ as a function of number of shots.

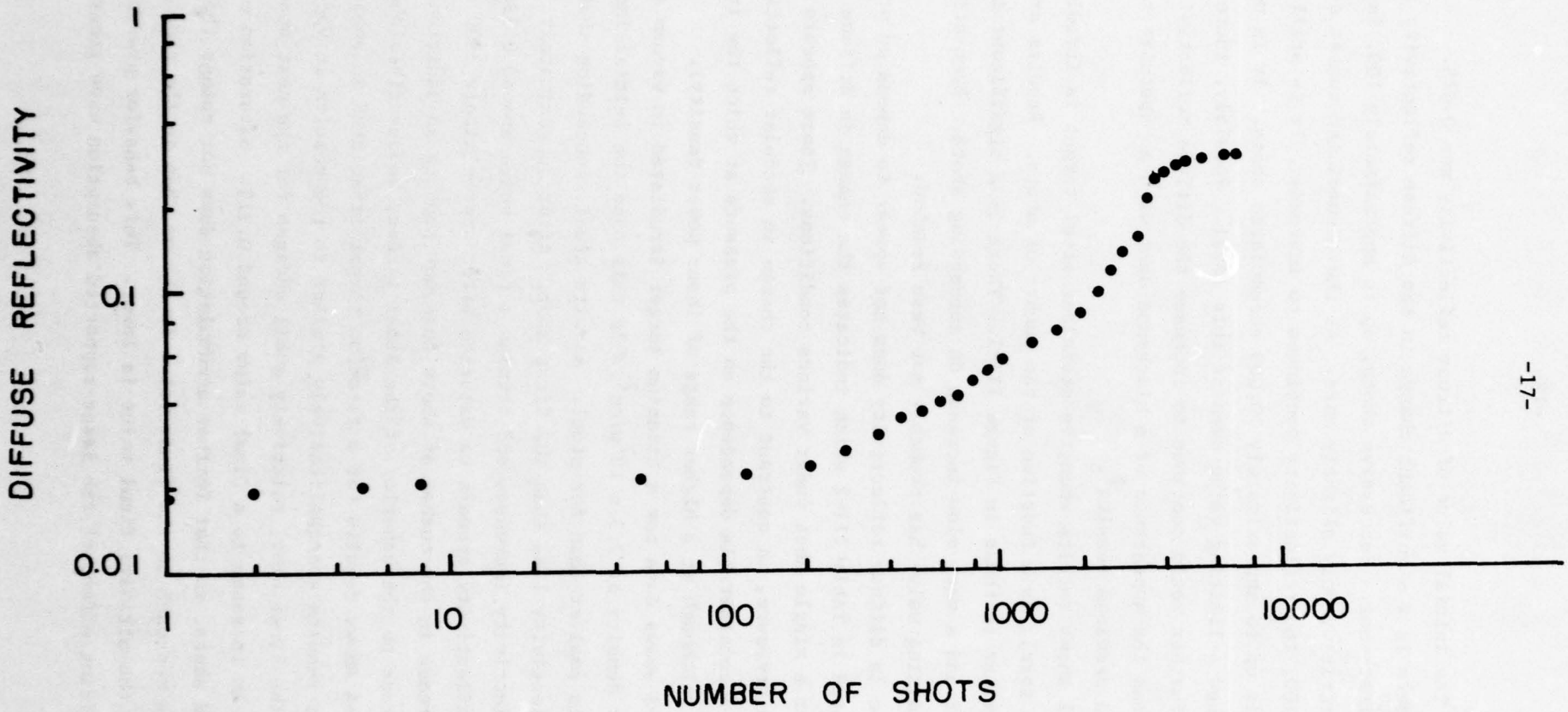

Figure III-4. Diffuse reflectivity at 0.5145μm for a titanium target irradiated in ambient air at a laser power density of $2.3 \times 10^7 w/cm^2$ as a function of number of shots.

$2.3 \times 10^7 w/cm^2$. The initial value of diffuse reflectivity was 0.025.

Therefore there is a significant change in the diffuse reflectivity in the visible on the first shot. Successive shots, up to approximately 100, increase the diffuse reflectivity only slightly more. As the accumulated number of shots increases above 100, the reflectivity continues to increase. It is still increasing rather irregularly up to approximately 10,000 accumulated shots. It is not clear that it has reached a limiting value even at this level. Possibly, increasing the number of shots further would continue to increase the diffuse reflectivity. The irradiated area has the appearance of a blackened spot with no specular reflectivity, in agreement with previous results[2].

Figure III-2 shows results when the stainless steel target is irradiated in ambient air (746 torr), as a function of the number of shots. Results are qualitatively similar to those in Figure III-1. There is a significant increase on the first shot and a very slow increase on succeeding shots. Even after almost 6000 shots, a limiting value has probably not been reached.

The increase in diffuse reflectivity does not appear to depend on pressure. This is illustrated in Table III-2 which indicates the change in diffuse reflectivity at $0.5145\mu m$ after a single shot under various conditions. There appears to be no dependence on pressure, in contrast to the change in specular reflectivity[2], which exhibited a considerable dependence on the pressure at which the irradiation was carried out (although at a higher range of laser power density).

Figure III-3 shows data for a titanium target irradiated in vacuum (0.03 torr) at a laser power density of $2.3 \times 10^7 w/cm^2$. In this case the initial increase on the first shot is smaller than for steel. As with steel, succeeding shots change the diffuse reflectivity less than the first shot. After approximately 100 shots, the diffuse reflectivity increases and attains a final value around 0.336. In this case the reflectivity appears to saturate after approximately 3000 shots, and further increase in the number of shots does not produce an additional effect. This is in contrast to the behavior of the steel target, as described above.

Figure III-4 shows results for a titanium target irradiated in ambient air (746 torr). The results are qualitatively similar to the results in vacuum. They show a jump on the first shot, relatively small changes for the next hundred shots or so, and then an increase to a final value around 0.312. Saturation occurs after several thousand shots, so that further accumulation does not change the final value much. The approach to the final value is slower than in the case of vacuum irradiation and the ultimate final value is lower. This behavior presumably is due to the shielding effect of the laser-supported absorption wave generated in

TABLE III-2

Diffuse Reflectivity at 0.5145μm.

Material	Conditions	Pressure (Torr)	Diffuse Reflectivity
Steel	Initial Value	--	0.025
Steel	1 shot, 2.3×10^7 w/cm^2	0.1	0.039
Steel	1 shot, 2.3×10^7 w/cm^2	300	0.036
Steel	1 shot, 2.3×10^7 w/cm^2	746	0.042
Titanium	Initial Value	--	0.011
Titanium	1 shot, 2.3×10^7 w/cm^2	0.03	0.015
Titanium	1 shot, 2.3×10^7 w/cm^2	746	0.018

the atmosphere above the target at one atmosphere pressure.

Some data for the change in diffuse reflectivity at 0.5145μm after a single shot as a function of laser power density are shown in Figure III-5, for a titanium target irradiated in air at 746 torr. Results indicate a threshold for damage around $1.5 \times 10^7 w/cm^2$.

We had originally planned to obtain time resolved data on the diffuse reflectivity at 9.6μm during the irradiation with the TEA laser. The interaction with the surface and the emission of the blowoff material were accompanied by a flash of white light, which saturated the detector. Therefore it was not possible to obtain measurements of the diffuse reflectivity during the time of the interaction. In our earlier measurements of specular reflectivity[2], we had avoided this problem by using a filter in front of the detector, so that only radiation in the narrow bandwidth region around 9.6μm, the wavelength of the probe laser beam, could reach the detector. This is not possible in the setup using the integrating ellipsoid, because radiation must be incident on the detector from a variety of angles. This precludes the use of an interference filter, which has transmission which is dependent upon the angle of incidence.

Data on the diffuse reflectivity after the irradiation are presented in Table III-3, and in Figures III-6 through III-9. The diffuse reflectivity for steel showed an increase after a single shot at a level around $3 \times 10^7 w/cm^2$. But no measurable increase was shown for a single pulse incident on a titanium target at this level. However, when a number of pulses were incident on the titanium target a cumulative effect was observed.

Figure III-6 shows data for the diffuse reflectivity at 9.6μm for a stainless steel target irradiated in ambient air at a laser power density of $3.2 \times 10^7 w/cm^2$. The diffuse reflectivity increases gradually but irregularly. In some regions, the increase is not monotoinic. At other places, there appears to be rather sharp increases for a small increment in the number of pulses. This behavior is accompanied by a change in the size of the spark above the surface. When there is a decrease in reflectivity, the spark also diminishes in intensity. We believe this may be accompanied by changes in the absorption characteristics of the surface, with an oxidized layer of the surface being formed and then temporarily being removed. This would account for behavior in which the diffuse reflectivity and the size of the spark decrease simultaneously. After several thousand shots, the reflectivity appears to saturate at a level above 90%.

Figure III-7 shows data for the stainless steel target irradiated in ambient air at a level of $2.3 \times 10^7 w/cm^2$. The change in diffuse reflectivity does not become

Figure III-5. Diffuse reflectivity at 0.5145μm for a titanium target irradiated in air by a single laser pulse, as a function of laser power density.

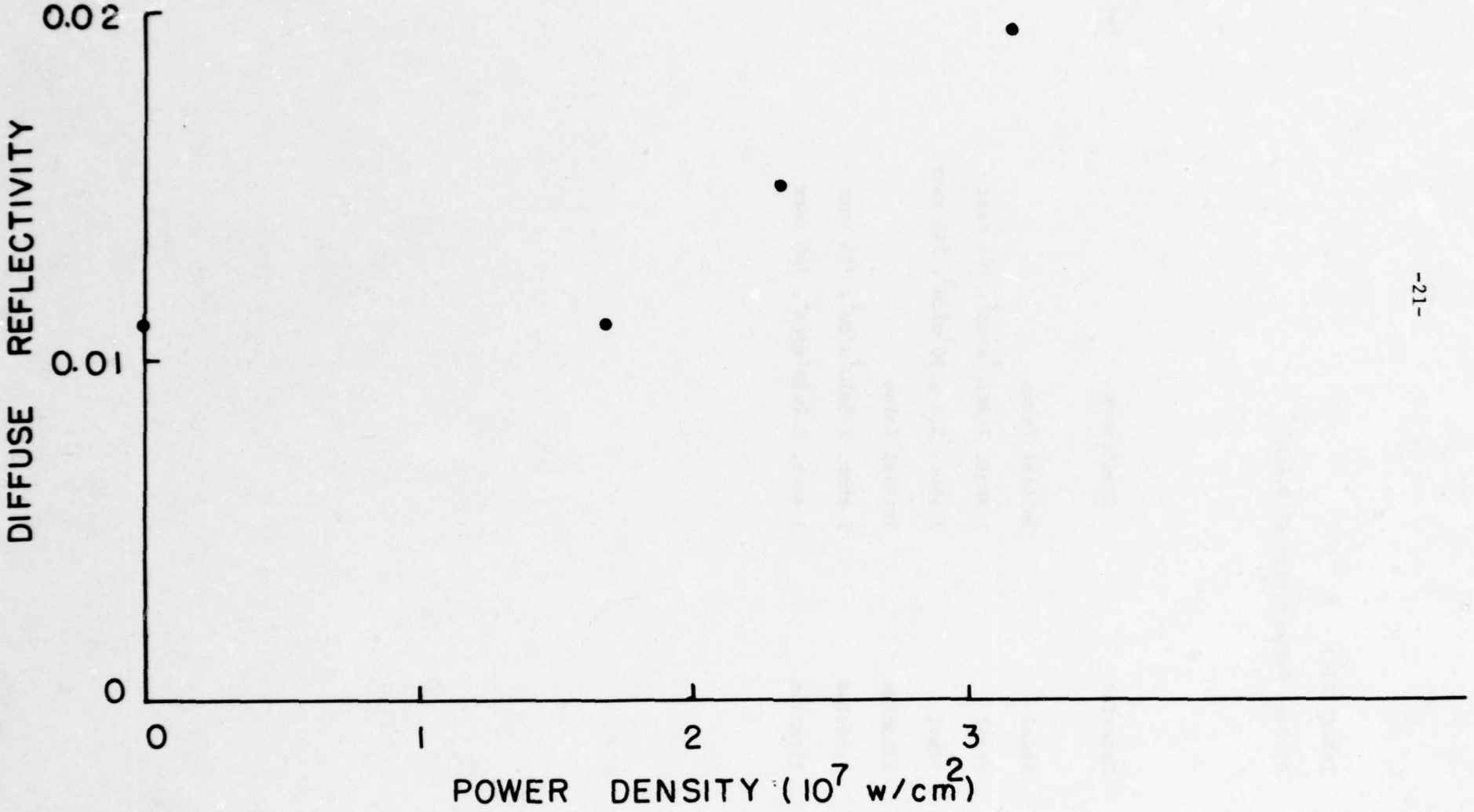

TABLE III-3

Diffuse Reflectivity at 9.6μm

Material	Conditions	Diffuse Reflectivity
Steel	Initial Value	0.119
Steel	1 shot, 2.3×10^7 w/cm^2, 746 torr	0.119
Steel	1 shot, 3.2×10^7 w/cm^2, 746 torr	0.132
Titanium	Initial Value	0.101
Titanium	1 shot, 2.3×10^7 w/cm^2, 746 torr	0.101
Titanium	1 shot, 3.2×10^7 w/cm^2, 746 torr	0.101

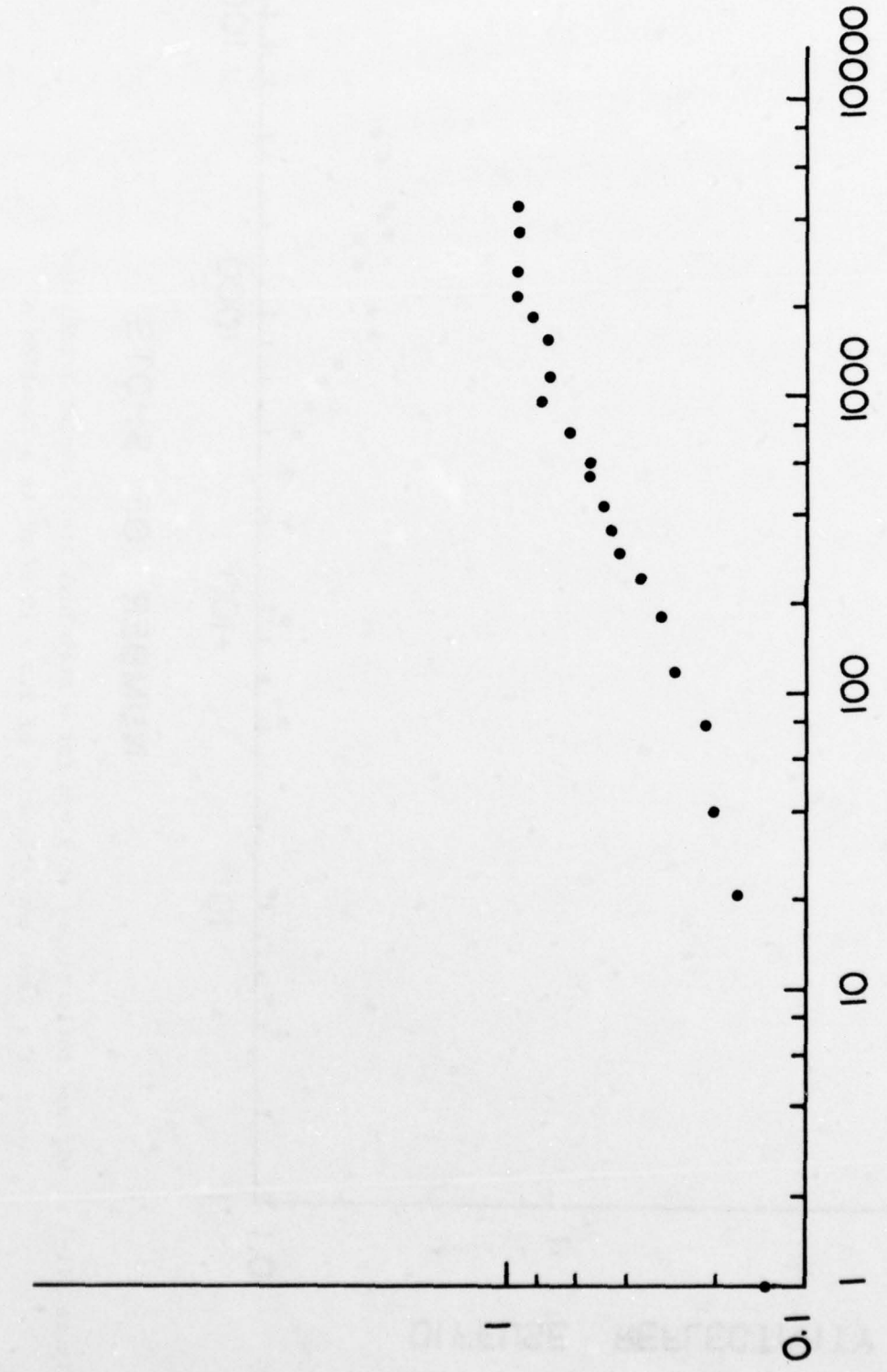

Figure III-6. Diffuse reflectivity at 9.6μm for a stainless steel target irradiated in air at $3.2 \times 10^7 w/cm^2$ as a function of number of shots.

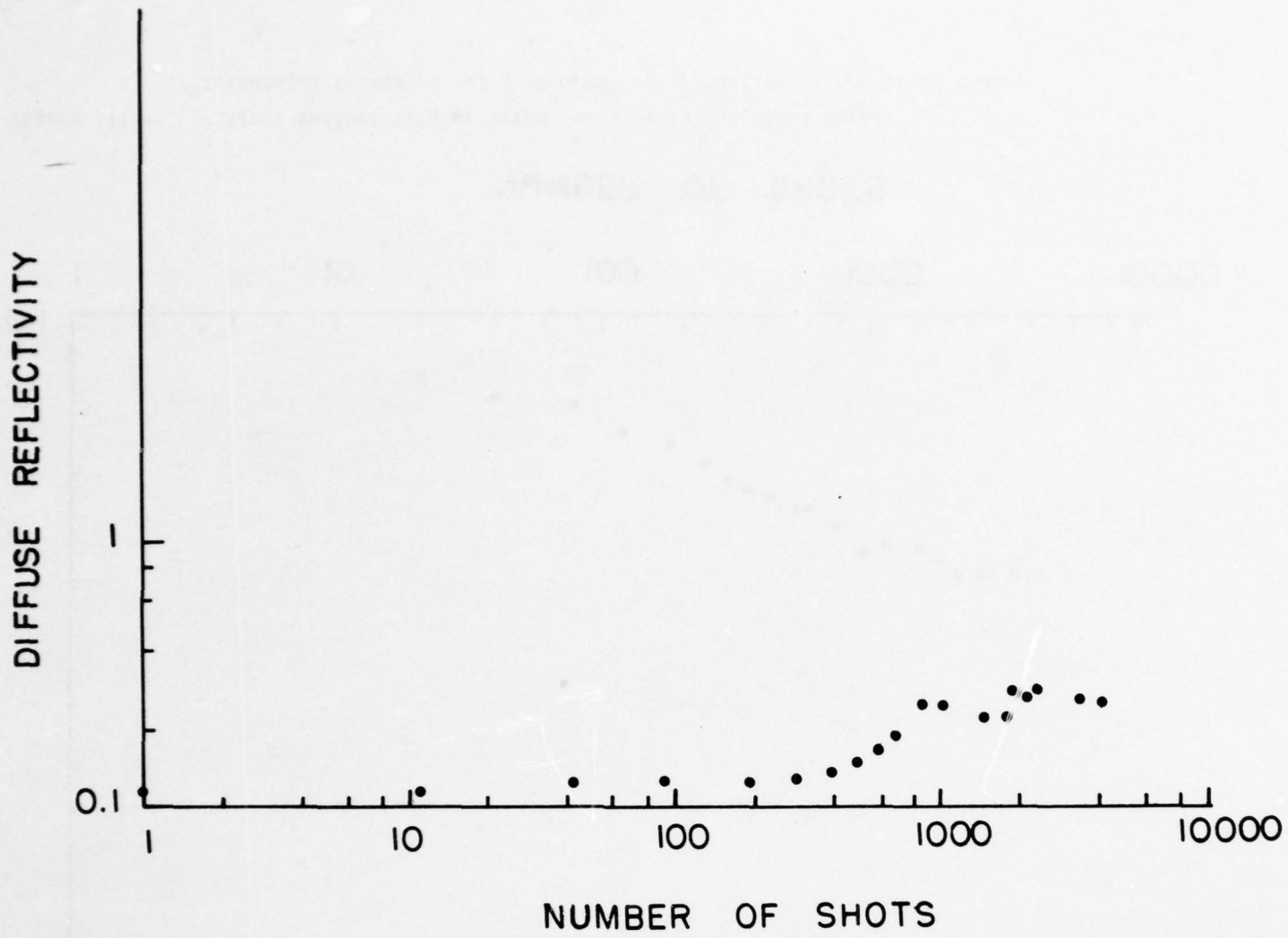

Figure III-7. Diffuse reflectivity at 9.6μm for a stainless steel target irradiated in air at a laser power density of $2.3 \times 10^7 w/cm^2$ as a function of number of shots.

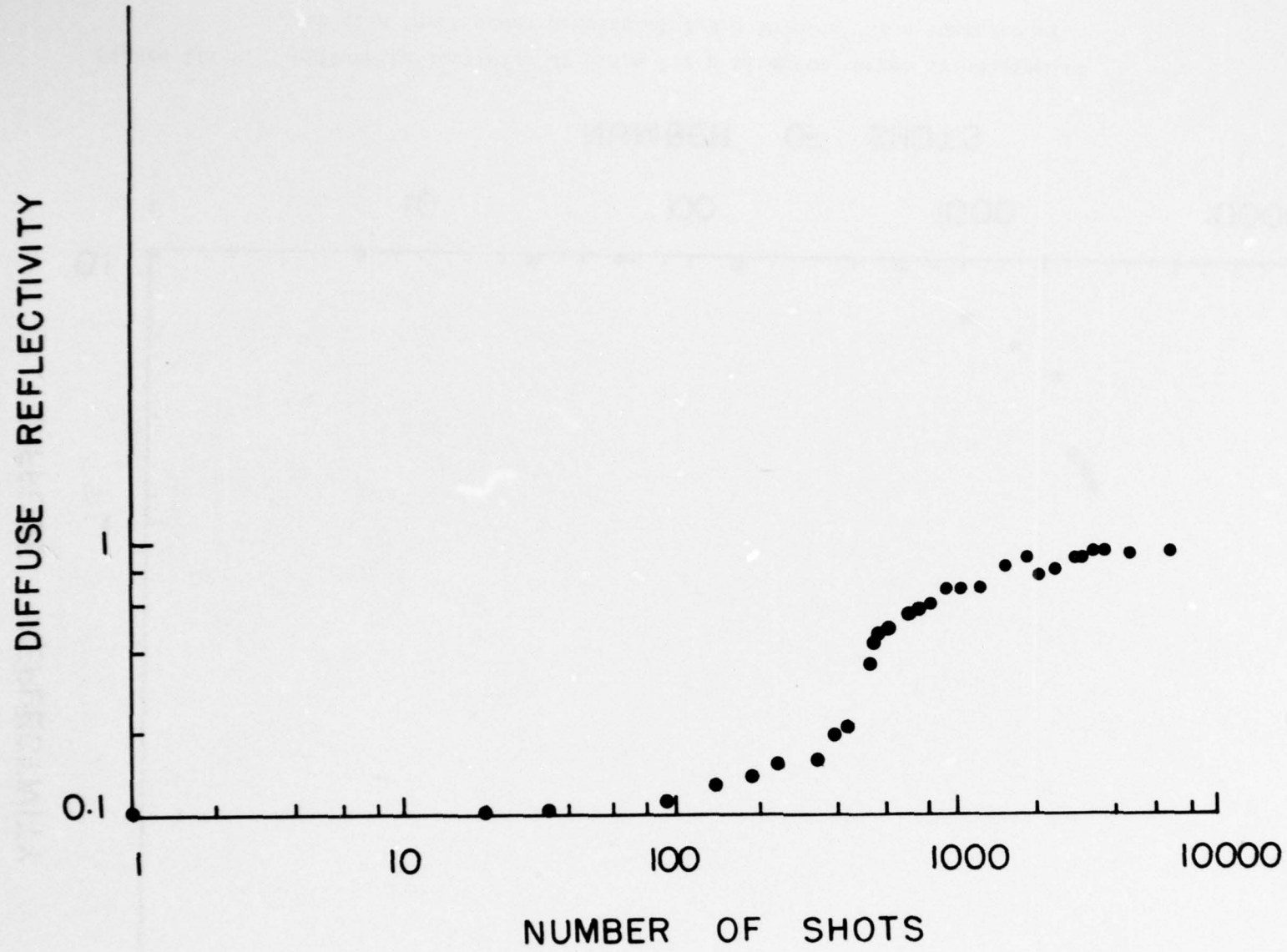

Figure III-8. Diffuse reflectivity at 9.6μm for a titanium target irradiated in air at 3.2 x 10^7w/cm^2 as a function of number of shots.

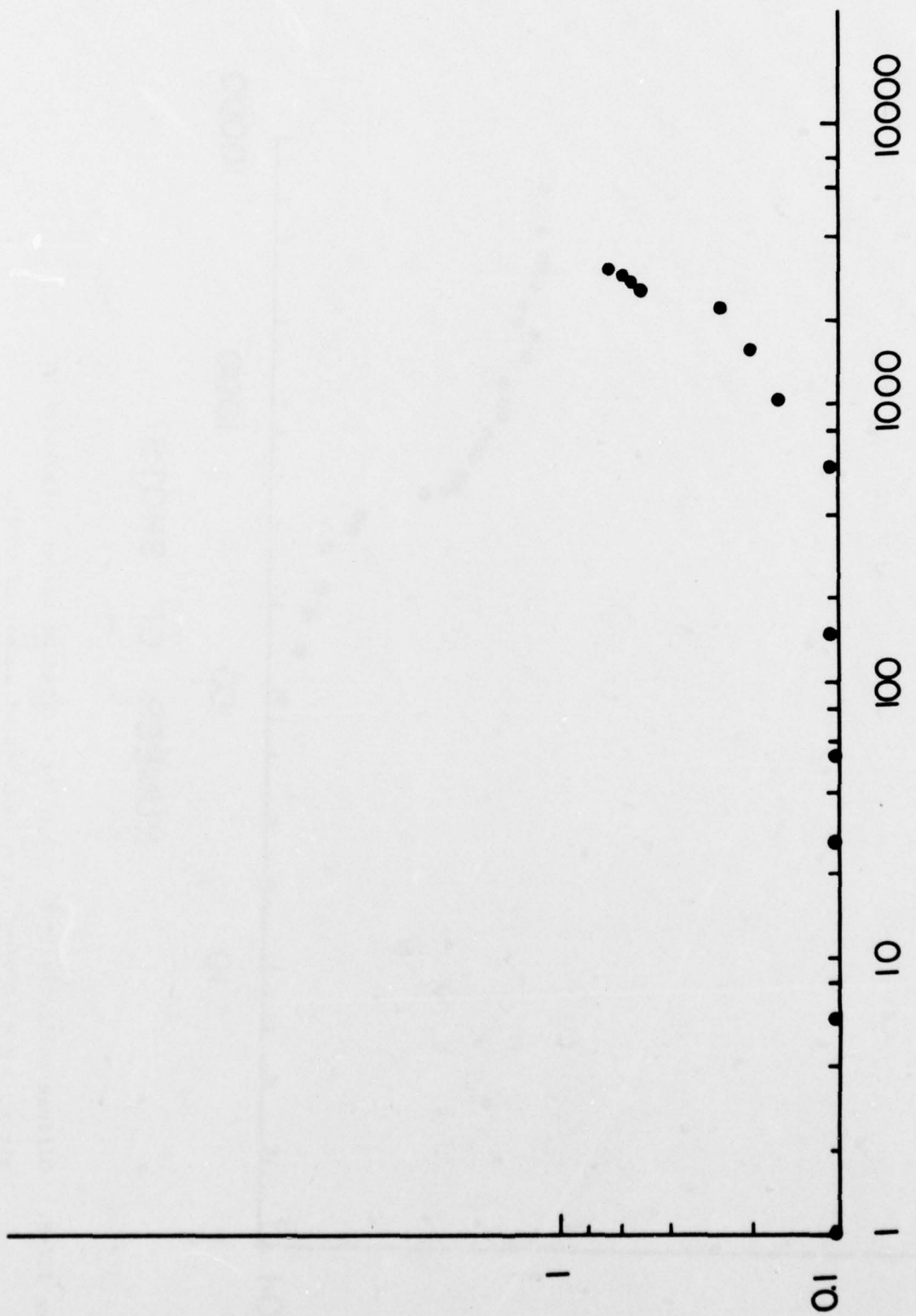

Figure III-9. Diffuse reflectivity at 9.6μm for a titanium target irradiated in air at a laser power density of 2.3×10^7 w/cm^2 as a function of number of shots.

apparent until several hundred shots are accumulated and then it increases gradually and irregularly. At this level of power density, even after several thousand shots it has apparently not reached a limiting value. Probably further shots would lead to a higher final value of reflectivity.

Figure III-8 shows the behavior of a titanium target irradiated in air at a laser power density of $3.2 \times 10^7 w/cm^2$. Under these conditions the first shot did not change the diffuse reflectivity at 9.6μm, even though there was a measurable effect on the diffuse reflectivity at 0.5145μm. In fact no measurable effect was noted until around 100 shots had been accumulated. The diffuse reflectivity then increased for several hundred shots. It then showed a sudden rapid increase near 500 shots. It then continued to increase till it reached the 90% level, at which point it saturated after several thousand shots.

The behavior with a slightly lower power density is similar, but it took longer for the reflectivity to begin to increase above its initial value. It did not begin to rise rapidly until after several thousand shots were accumulated. The results, shown in Figure III-9, indicate that it is still increasing after several thousand shots and presumably would continue to increase to a higher value for a larger number of shots.

Although time-resolved data could not be obtained directly, we inferred some values from the final value of diffuse reflectivity after a single shot. We know the initial value of the reflectivity and the final value, and we know the time behavior of the specular reflectivity[2]. If we assume that the change between the initial and final values has the same time dependence as the change between the initial and final values of the specular reflectivity as measured earlier, we may infer a change in the diffuse reflectivity as a function of time. Then we may plot the absorptivity as a function of time, as indicated in Figure III-10. This gives the derived absorptivity as a function of time for a stainless steel target irradiated in vacuum for two conditions of laser power density, as obtained using the assumptions described above.

In Table III-4, we present data on the final value of absorptivity after irradiation under various conditions as indicated.

We had also intended to obtain data on the effect of varying pulse repetition rate, with interpulse times in the microsecond region. Performance of this task depended on borrowing a second CO_2 TEA laser from the Honeywell Systems and Research Center. The two lasers could be triggered independently to provide variable interpulse times shorter than those available from a single TEA laser. The work schedule at the Honeywell Systems and Research Center precluded borrowing of this laser during the current contract period, so we were unable to accomplish this planned task.

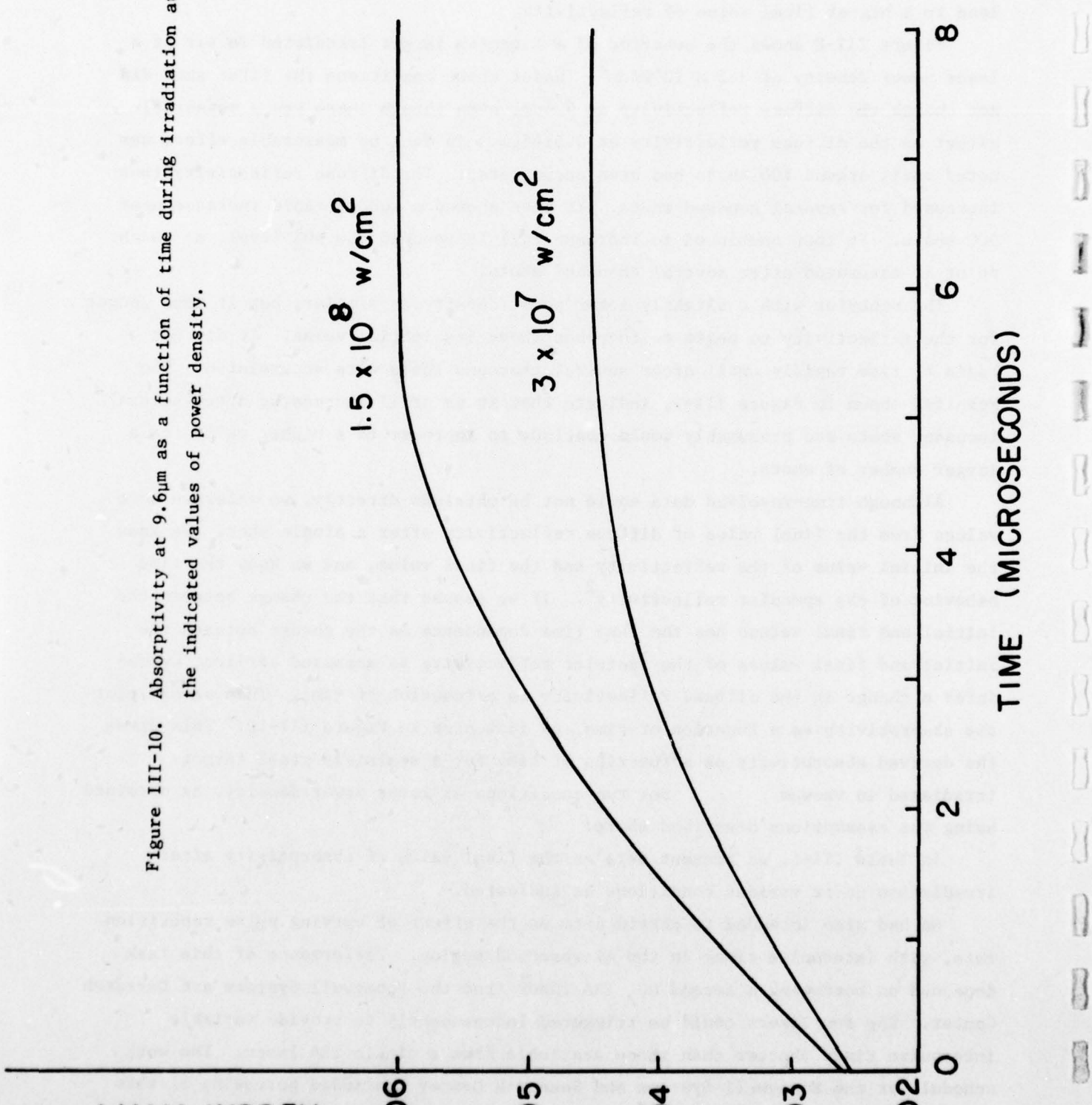

Figure III-10. Absorptivity at 9.6μm as a function of time during irradiation at the indicated values of power density.

TABLE III-4

Absorptivity at 10μm

Material	Conditions	Absorptivity
Steel	Initial Value	0.025
Steel	1 shot, Vacuum, 2.3×10^7 w/cm^2	0.045
Steel	1 shot, Vacuum, 1.5×10^8 w/cm^2	0.060
Steel	5835 shots, Air, 2.3×10^7 w/cm^2	0.280
Titanium	Initial Value	0.014
Titanium	1 shot, Air, 2.3×10^7 w/cm^2	0.092
Titanium	6780 shots, Air, 2.3×10^7 w/cm^2	0.313
Titanium	130 shots, Air, 3.2×10^7 w/cm^2	0.092

In summary, we determined the effect of the CO_2 TEA laser radiation on the diffuse reflectivity of metallic surfaces, under varying conditions of irradiation. The results are compatible with the effect being due to melting of the surface, with flow and redistribution of the material so as to provide a diffusely reflecting surface. The initial highly specularly reflecting surface is eroded, so that a pattern of small hills and valleys is formed, with dimensions of the order of a few micrometers. Thus the initial effect on the visible reflectivity is more pronounced than the initial reflect on infrared reflectivity, as indicated in Tables III-2 and III-3. As the accumulated number of shots increases, the surface continues to oxidize and blacken, so that it becomes a highly diffusely reflecting surface, with increased values of absorptivity.

SECTION IV
PRESSIRE PULSES

At sufficiently high values of laser power density, an absorbing plasma is ignited in the atmosphere in front of the target surface. The plasma moves back up the laser beam toward the laser, as a laser-supported absorption wave. It shields the target surface and absorbs much of the incident energy. The hot expanding plasma also exerts pressure on the surface, which leads to both an impulsive motion of the target as a whole and also to shock waves which propagate supersonically within the target. If the shock pressure is high enough, the target may crack or spall. The study of the shock pressure coupled into the target provides an important tool for investigation of the coupling of the laser energy to targets. We have carried out a parametric study of the shock pressure as a function of variable conditions of irradiation. Much of this work has already been described in a previous interim report[4]. However, a portion of the work continued into the present contract period. Therefore we shall describe the entire investigation in this report, so as to make the final report self-contained. Thus this section will repeat some material already described in an interim report.

The experimental arrangement uses an interferometric system shown in Figure IV-1. The TEA laser pulse is focussed on the front surface of the target. The resulting laser-supported absorption wave produces a pressure pulse which propagates into the target as a shock front. When the shock front reaches the rear surface of the target, it is reflected and the rear surface moves in response to the reflection of the shock front. The motion is measured by determining the velocity of the fringes in the Michelson interferometer, for which the rear surface of the target serves as one of the mirrors. The rear surface is polished to a specularly-reflecting finish. The helium-neon laser used in the interferometer (Spectra-Physics model 120) has an output of 5 milliwatts distributed among several longitudinal modes. Because the path differences in the two arms of the interferometer can be matched closely, it is not necessary to employ a single-frequency helium-neon laser. The motion of the fringes is detected by a planar diffused silicon diode (United Detector Technology PIN-3D) with a quoted response time of 15 nanoseconds. A diverging lens in the detector arm of the interferometer is adjusted so that one fringe of the interference pattern falls across the diode aperture, so as to maximize the signal level corresponding to passage of one fringe across the detector.

When the rear surface of the target moves by one-half the wavelength of helium-neon laser light, one complete fringe in the interferometer will move across

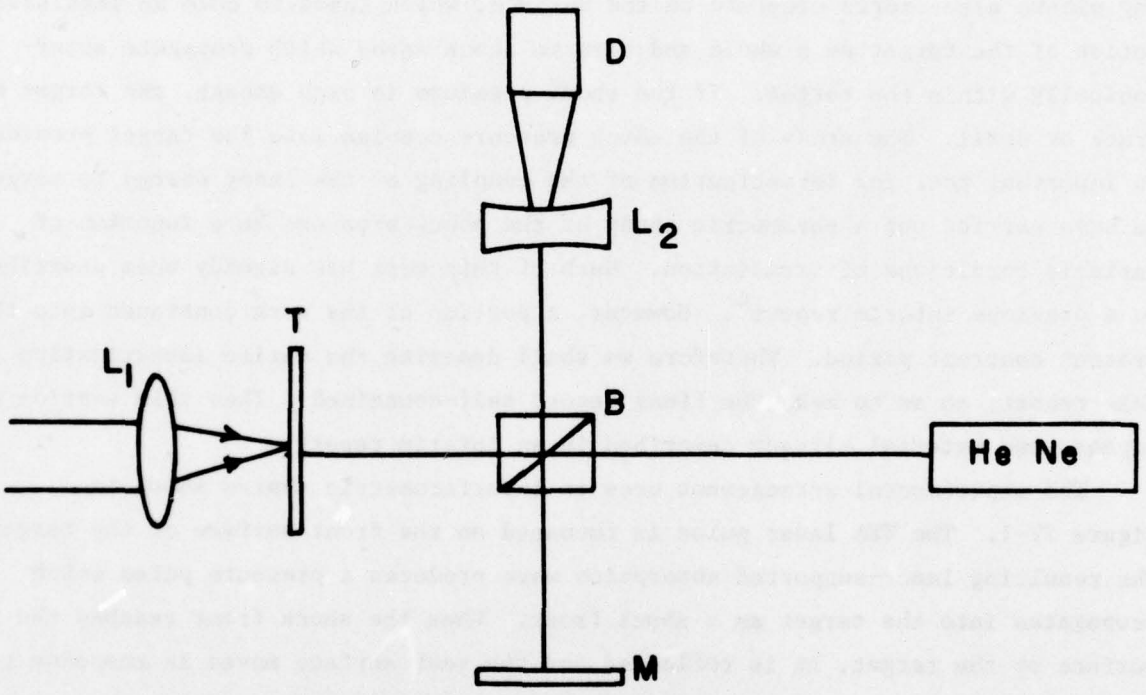

Figure IV-1. Interferometric arrangement for measurement of pressure pulses. The TEA laser beam is incident from the left. L_1 is a lens that focusses the beam on the target T. The helium-neon laser beam passes through the beam splitter B. The two mirrors in the Michelson interferometer are indicated as the mirror M and the rear surface of the target. The lens L_2 diverges the beam so that one fringe falls on the aperture of the detector D.

the face of the detector. The target surface velocity can be determined from the amplitude modulation of the fringe pattern. From measurements of the rear surface velocity of the target, the pressure in the shock front which caused the motion can be determined[7]. Because the events occur in a microsecond time frame, low frequency motion of the fringes, produced by factors such as building vibrations, does not influence the results.

The target is mounted on a micrometer-driven pedestal inside a vacuum chamber with Irtran 2 windows. This allows measurements of the shock pressure as a function of the nature of the ambient gas and its pressure. The micrometer motion allows presentation of fresh target areas for irradiation. The entire bell jar can be evacuated to a minimum pressure around 0.01 torr.

Figure IV-2 presents data on the shock pressure as a function of time for irradiation of a stainless steel (300 series) target of thickness 0.6mm, for a laser power density of $1.26 \times 10^8 w/cm^2$. The peak shock pressure is observed several hundred nanoseconds after the start of the laser pulse. The pressure decreases to zero after 3μs. The error bar indicates only the uncertainty due to fringe counting. Structure due to reflection of the shock front between the target surfaces may be present, but the scatter in the data makes this difficult to determine.

A question arises about the planar nature of the shock front propagating through the target. The target was thinner than the approximately 1 millimeter transverse dimension of the laser beam at the front surface. Measurements made as a function of distance from the center of the beam on the rear surface of the target indicate a rapid decrease of shock pressure as one moves out from the radial center of the shock. Thus it is reasonable to assume a planar nature for the shock.

In addition, measurements made as a function of target thickness indicate that the peak shock pressure is attenuated by approximately 20% in transmission through 0.6mm inches of target material. Thus extrapolation of the shock pressure back to the front surface would indicate a peak pressure around 130 bars at the front surface.

The data presented in the remaining portion of the paper will describe results for the peak value of pressure observed, that is the value at the beginning of the measured shock pressure when the shock front reaches the rear surface. The values presented are rear surface values, which would be approximately 20% lower than the front surface values.

Figure IV-3 shows measurements for the shock pressure as a function of ambient air pressure, for the two different conditions of laser pulse duration, as described above. These data are relevant to an aluminum target (2017 alloy) 0.6mm

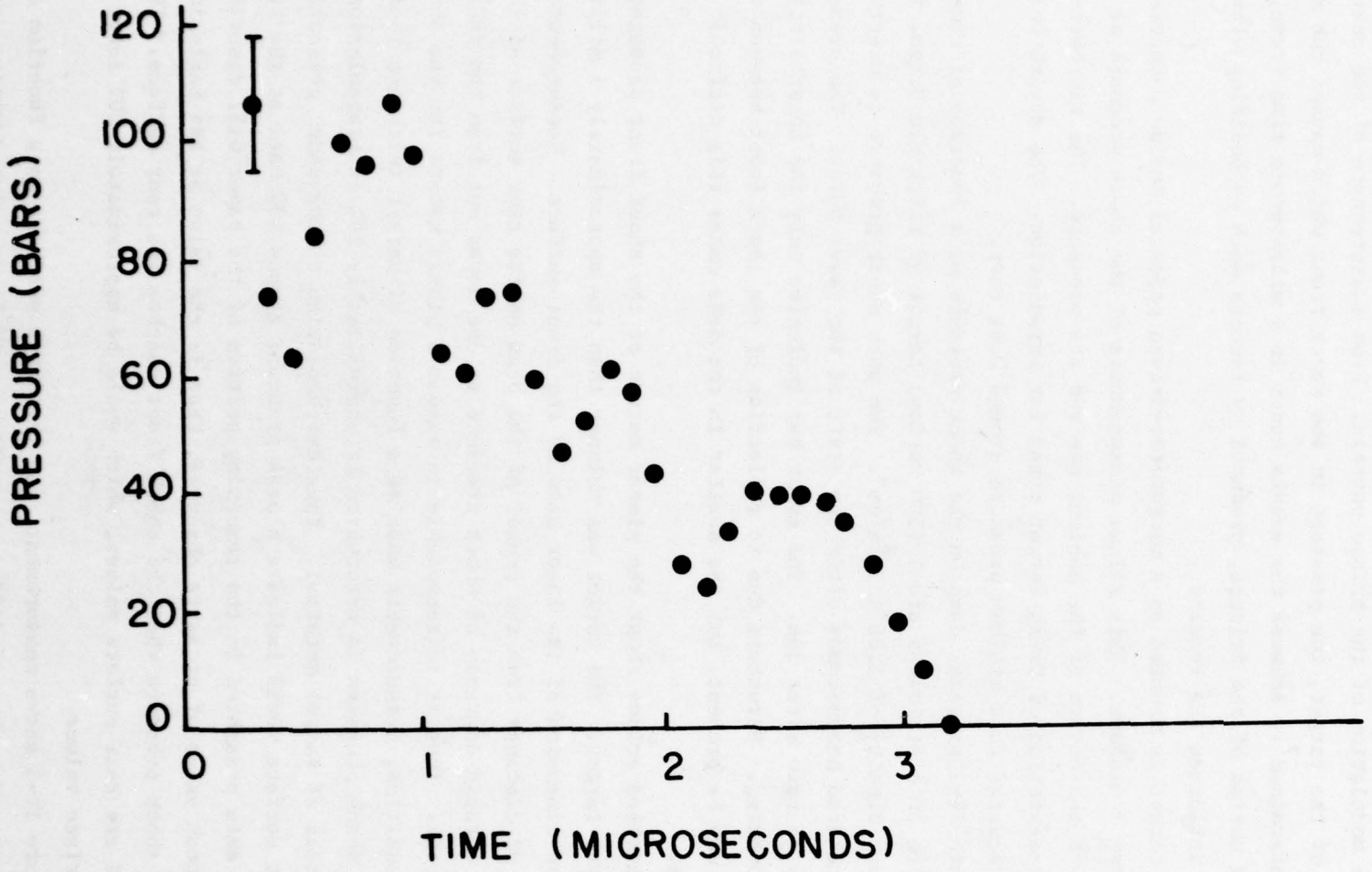

Figure IV-2. Pressure as a function of time after the start of the laser pulse for a steel target irradiated in air at 1 atmosphere pressure.

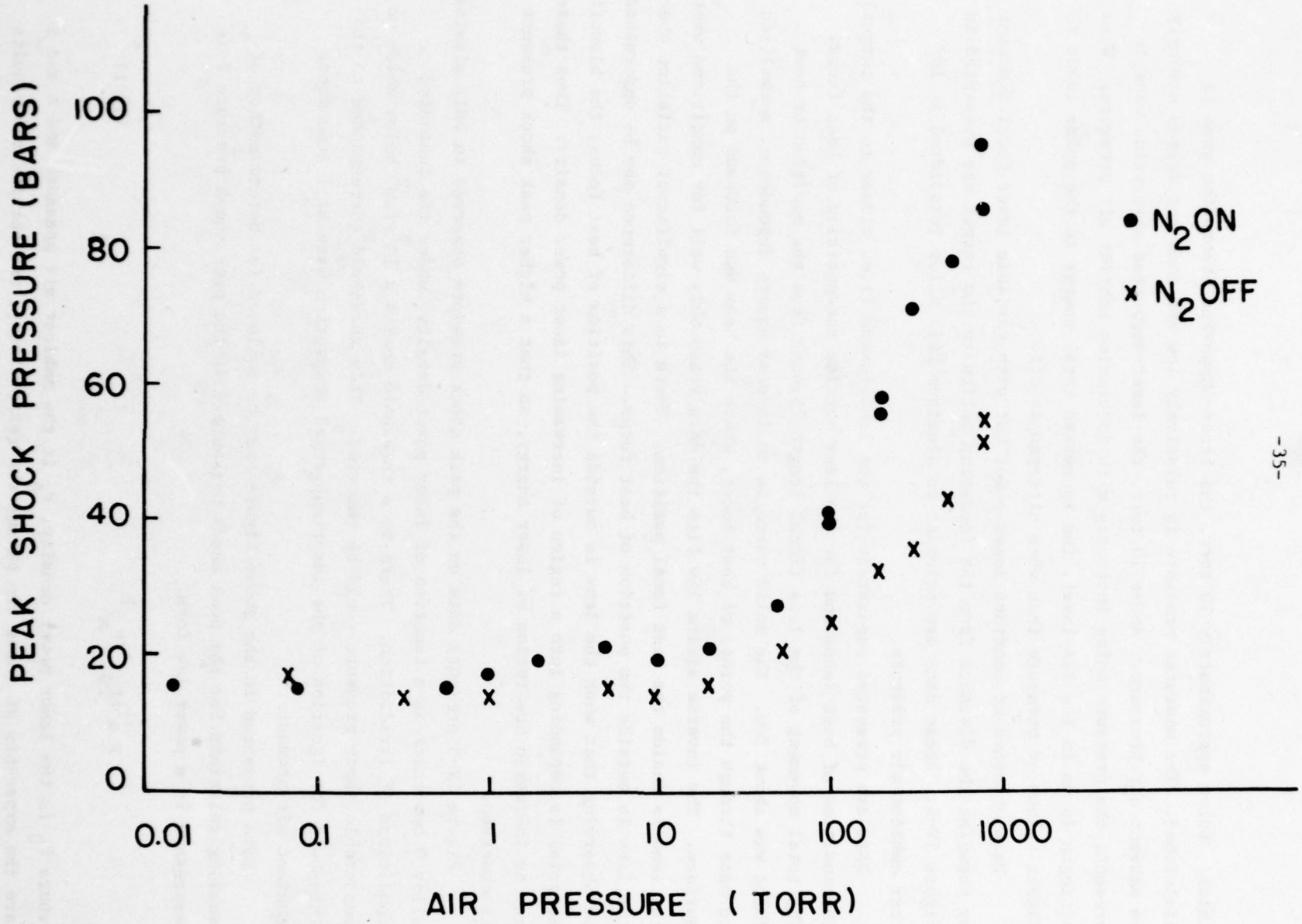

Figure IV-3. Peak shock pressure as a function of ambient air pressure for an aluminum target irradiated at $1.26 \times 10^8 w/cm^2$.

thick. Below approximately 10 torr, the laser-supported absorption wave is diminished. The measured pressure is relatively low and does not depend strongly on ambient air pressure. Above 10 torr, the laser-supported absorption wave is present; the pressure pulse increases with increasing ambient air pressure. When nitrogen is on in the TEA laser, the increased total energy in the pulse leads to higher values of pressure than when nitrogen is off.

Data obtained at constant laser power but with variable laser focal diameter by changing the distance from the focussing optics to the target are presented in Figure IV-4. These data are relevant to aluminum 2017 alloy irradiated at 100 torr ambient air pressure.

Data are presented separately for the lens inside (i.e. closer to the target) the position of best focus and for the lens outside the position of best focus. The total movement of the lens (focal length 25.4cm) from the position of best focus was about 3cm. The solid curve is an inverse square dependence, normalized to pass through the points of best focus, where the beam was focussed on the surface. The inverse square law fits the data reasonably well for conditions where the lens is inside the best focal position. There is a significant variation when the lens is outside the position of best focus. This difference may be understood by observing that when the lens is outside the position of best focus, the blowoff material is expanding into a region of increasing laser power density. Thus there may be increased absorption of laser energy, so that a higher peak shock pressure is observed.

Figure IV-5 presents data on the peak shock pressure observed in 2017 aluminum alloy 0.6mm thick as a function of laser power density, under the indicated conditions of irradiation. There is a threshold near $4 \times 10^7 w/cm^2$ below which no measurable shock pressure could be observed. This threshold corresponded to the threshold for ignition of the laser-supported absorption wave at 1 atmosphere ambient air pressure.

Data presented in the above figures may be employed for determination of scaling relations for the peak shock pressure. If the peak shock pressure P is expressed in a power law form:

$$P \propto (P_0)^A (P_A)^B \qquad \text{(IV-1)}$$

where P_0 is the laser power density, P_A is the ambient air pressure and A and B are the exponents of these two parameters respectively, one obtains the results shown in Table IV-1 for a least squares fitting to the data for aluminum 2017 alloy. Table IV-1 also shows values for A and B derived from a model of the inter-

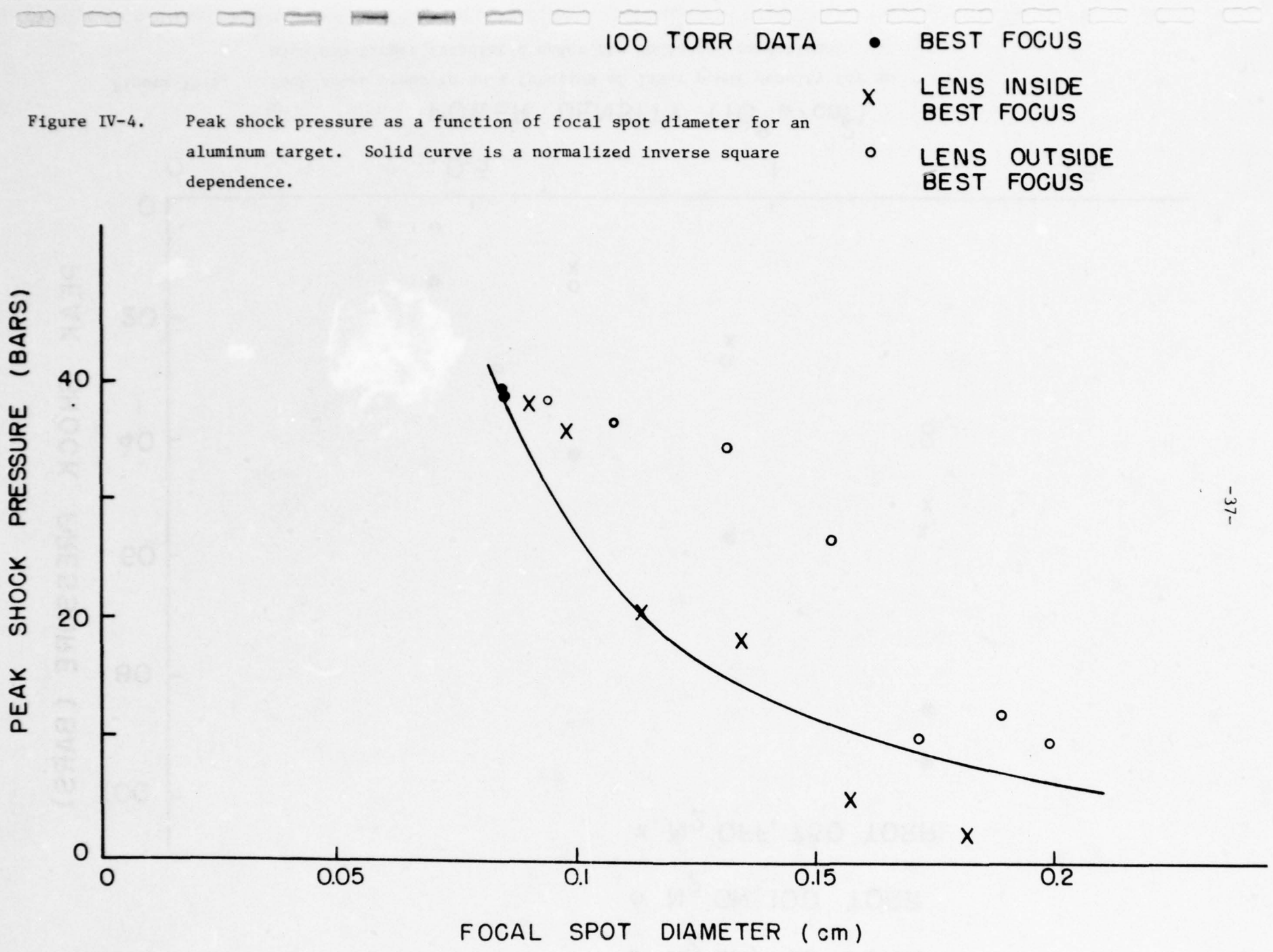

Figure IV-4. Peak shock pressure as a function of focal spot diameter for an aluminum target. Solid curve is a normalized inverse square dependence.

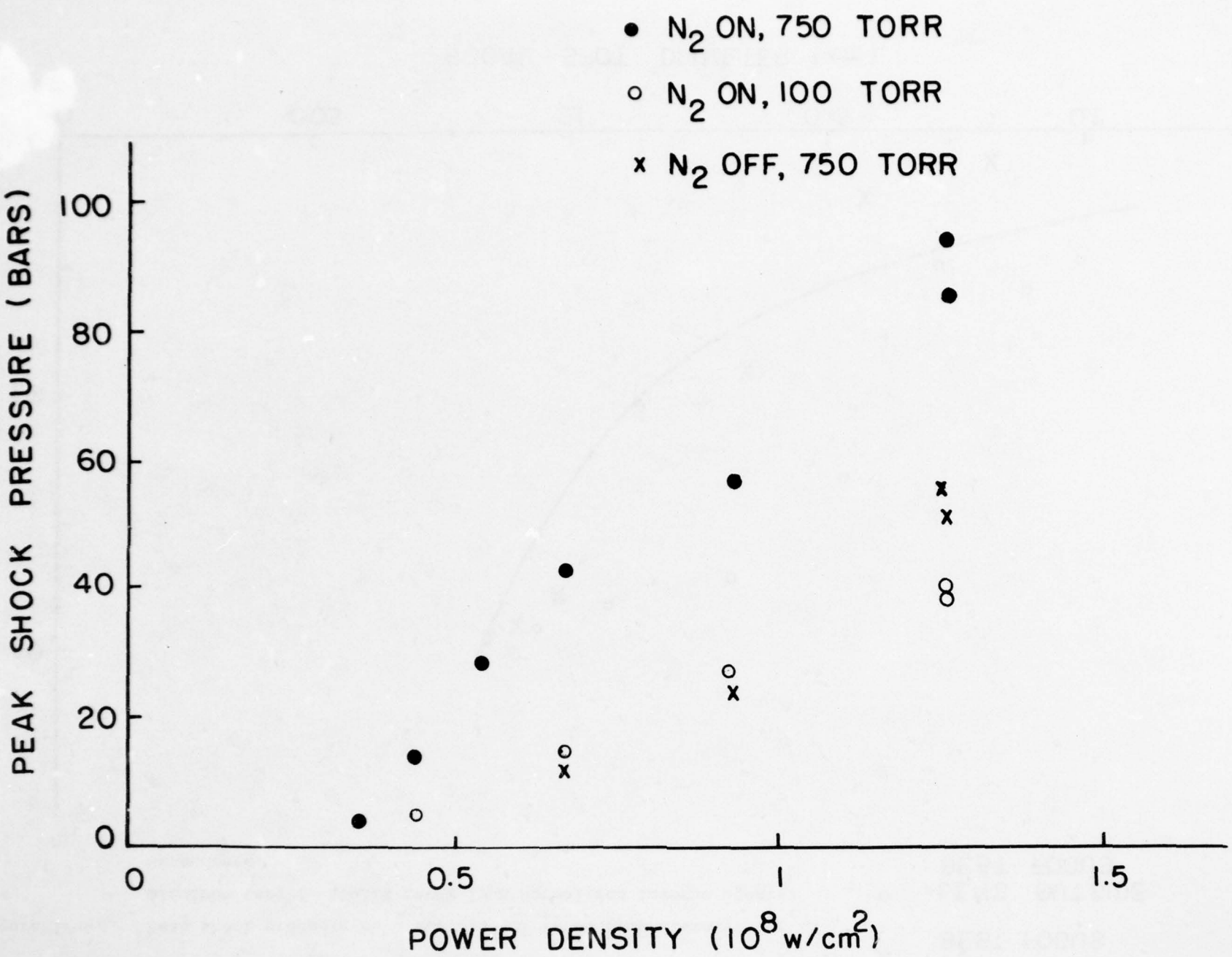

Figure IV-5. Peak shock pressure as a function of laser power density for an aluminum target irradiated under the indicated conditions.

TABLE IV-1

Exponents in Scaling Relation, Equation IV-1.

	Nitrogen On		Nitrogen Off	
	A	B	A	B
Least Squares Fit to Data	0.89	0.51	1.14	0.47
Semi-empirical Model	0.97	0.61	1.08	0.53

action. The model is based on the cylindrical blast wave model of Pirri[8] but modified by the empirically observed absorption in the blowoff material as a function of the variable parameters. Thus, Pirri's model predicts a dependence of the form:

$$P \alpha P_0^{2/3} P_A^{1/3} \qquad \text{(IV-2)}$$

It assumes essentially complete absorption of the incident laser energy in the plasma. Because a substantial fraction of the incident laser energy is transmitted under the present experimental conditions, the model has been modified so as to include only energy actually deposited in the blowoff plasma. Only the absorbed energy will be effective in driving the laser-supported absorption wave and in coupling pressure to the surface. The absorbed laser power density P_{oa} as a function both of the incident laser power density and of the ambient air pressure has been observed experimentally to scale as:

$$P_{oa} \alpha (P_{oi})^{1.46} (P_A)^{0.415} \qquad \text{(IV-3)}$$

where nitrogen is on in the laser, and as:

$$P_{oa} \alpha (P_{oi})^{1.62} (P_A)^{0.20} \qquad \text{(IV-4)}$$

where nitrogen is off. In the above equations, P_{oi} is the incident laser power density. This modeling therefore is semi-emperical; it avoids the difficult problems of trying to calculate ab initio the absorption in the blowoff material.

The results presented in Table IV-1, based on a modified cylindrical blast wave, appear in reasonably good agreement with the experimental results. A similar fitting attempted using a spherical blast wave was less successful. This is in contrast to results obtained for impulse measurements[5] performed under similar circumstances. For that case, a modeling based on a spherical blast wave gave a better fit.

Another recent model developed by Pirri[9] indicates scaling of shock pressure with laser power density as the seven-ninths power, a result which is in reasonable accord with the experimental results presented in Table IV-1. However, if this model, which assumes absorption of all the incident radiation, is modified to account for partial absorption, then one obtains scaling as the 1.14 power, with nitrogen on in the laser, a result rather higher than the observed value. This model is probably more applicable in a higher regime of laser power density, where

the incident energy would be substantially completely absorbed.

To compare different materials on a consistent basis, Table IV-2 presents data for all the metallic materials for which pressure has been measured, reduced to a constant value of laser power density of $1.2 \times 10^8 w/cm^2$. Values had been obtained for three different thicknesses of aluminum targets as indicated. The zero thickness value is the extrapolated value as discussed above. These results are all for irradiation at one atmosphere ambient pressure. We observe that the values do not vary greatly between different materials under comparable conditions of irradiation, indicating once again the dominant role of the laser-supported absorption wave in producing the shocks.

TABLE IV-2

Values of Peak Pressure (Bars)

($1.2 \times 10^8 w/cm^2$)

Material	Thickness				
	0	0.025 in.	0.043 in.	0.050 in.	0.2 in.
Aluminum	112*	90		64	6.6
Stainless Steel			70		
Titanium				68	

*Extrapolated

Now let us consider potassium chloride, an important material for laser windows and a material for which mechanisms of laser damage are important. Under the present conditions of irradiation, potassium chloride may be substantially damaged by the laser irradiation. We measured the shock pressure in single crystalline potassium chloride (Harshaw) and obtained results shown in Figure IV-6 for the peak shock pressure as a function of laser power density, for irradiation in ambient air at one atmosphere pressure. The rear surface of the sample was gold-coated in order to form the mirror surface for the interferometer. The values of peak shock pressure are considerably lower than those that would have been observed for metallic samples under the same conditions of irradiation. Thus at a power density around $7 \times 10^7 w/cm^2$, we would have expected a shock pressure around 40 to 50 bars in a aluminum sample.

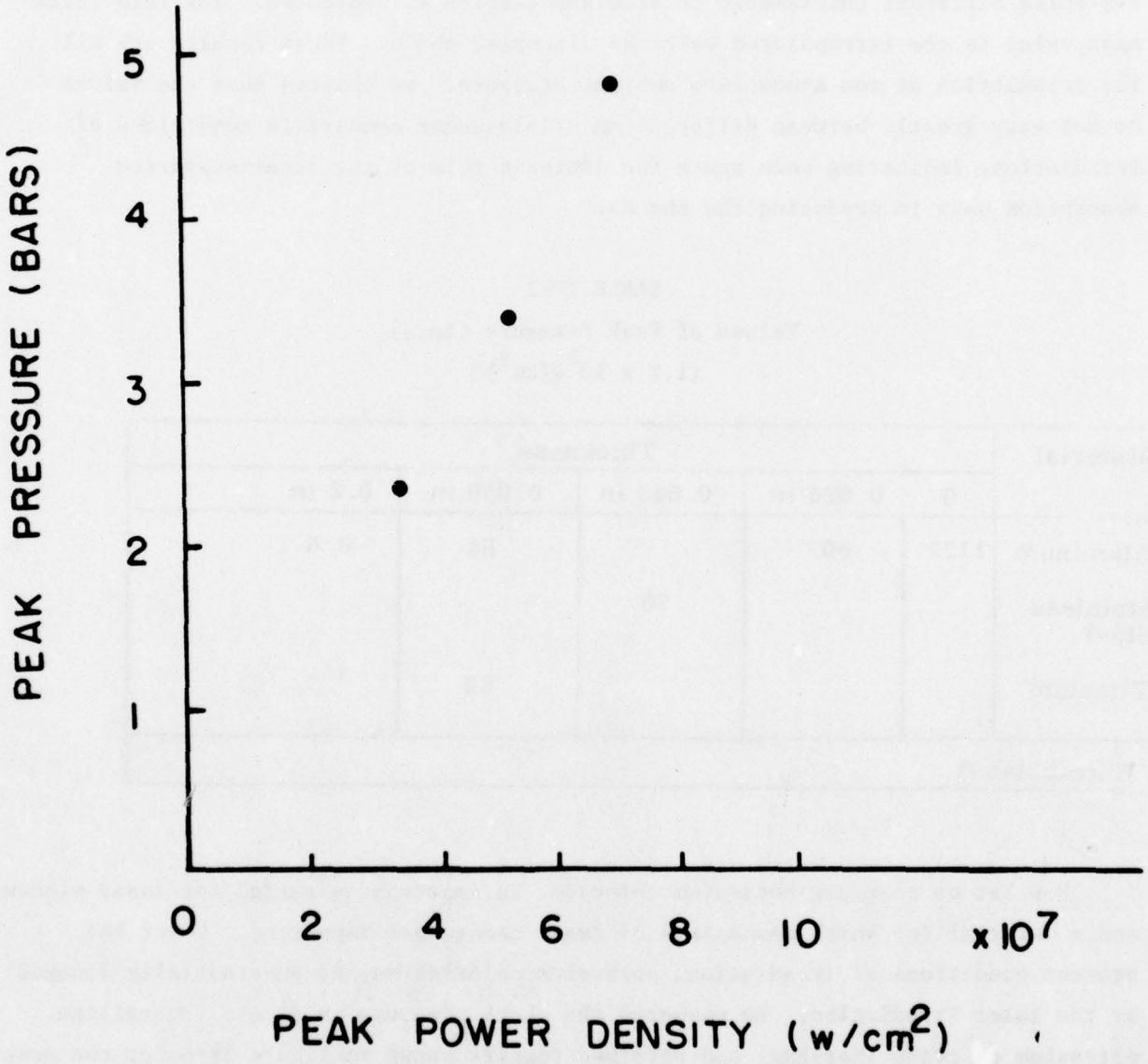

Figure IV-6. Peak shock pressure as a function of laser power density for a potassium chloride target.

We note that the potassium chloride samples were significantly damaged by the irradiation, whereas the pressures involved were considerably below the damage threshold for the metallic samples. No fracturing or spalling was observed in metallic samples. The difference of observed pressure values with the single crystalline potassium chloride samples is due to expenditure of the energy in cracking and damage of the sample. For the results in Figure IV-6, there is a threshold slightly below $4 \times 10^7 w/cm^2$. This corresponds to the threshold at which a measurable pressure pulse is observed. It also corresponds to the threshold for ignition of a laser-supported absorption wave. A comparison is shown in Table IV-3. The threshold for observation of a measurable pressure pulse also corresponds to the threshold for observation of threshold surface cracking, which is shown in Figure IV-7. The surface shows cracks on cleavage planes of the single crystalline material, with initiation at small sites of imperfections from which a small amount of material removal may be observed.

We also observed an effect reported previously[10] where preconditioning at lower values of laser power can increase the damage threshold. With preconditioning, the threshold for observation of a pressure pulse corresponded to this increased damage threshold. The preconditioning technique involved firing the laser a number of times at values below the damage threshold. The laser power is gradually until the damage threshold is reached. The values obtained in this way exceed values found when the first pulse on an area is at full power. With preconditioning, the gold coating on the rear surface is partially removed and the values observed for pressure pulses must be considered to be less reliable. However during this procedure the threshold for observation of a measurable pressure pulse did increase to the same value as the damage threshold.

In addition polycrystalline potassium chloride (Honeywell material) exhibited a considerably higher threshold for laser damage then did single crystalline material. No data are available for pressure pulses in this material. The phenomenology indicated by Table IV-3 and Figure IV-7 shows that fracture begins at the sites of imperfections on the surface. If the imperfections are removed at relatively low laser power density, without producing a laser-supported absorption wave and without producing a shock front which will fracture the material, the damage threshold increases markedly. These results are of interest because of the importance of alkali halide material as windows for high power lasers.

Figure IV-8 shows a scanning electron microscope photograph of the damage resulting from irradiation of the single-crystalline potassium chloride at levels well above threshold. Extensive damage is revealed. The original crater contained pulverized rubble fractured along cleavage planes of the crystal, which was removed

TABLE IV-3

Thresholds Relevant to Potassium Chloride

Single-Crystalline Material	
Observation of shock pressure (1st shot)	$3.6 \times 10^7 w/cm^2$
Surface damage (1st shot)	$3.6 \times 10^7 w/cm^2$
Observation of shock pressure (with preconditioning)	$6.4 \times 10^7 w/cm^2$
Surface damage (with preconditioning)	$6.4 \times 10^7 w/cm^2$
Polycrystalline Forged Material	
Surface Damage (1st shot)	$>3 \times 10^8 w/cm^2$

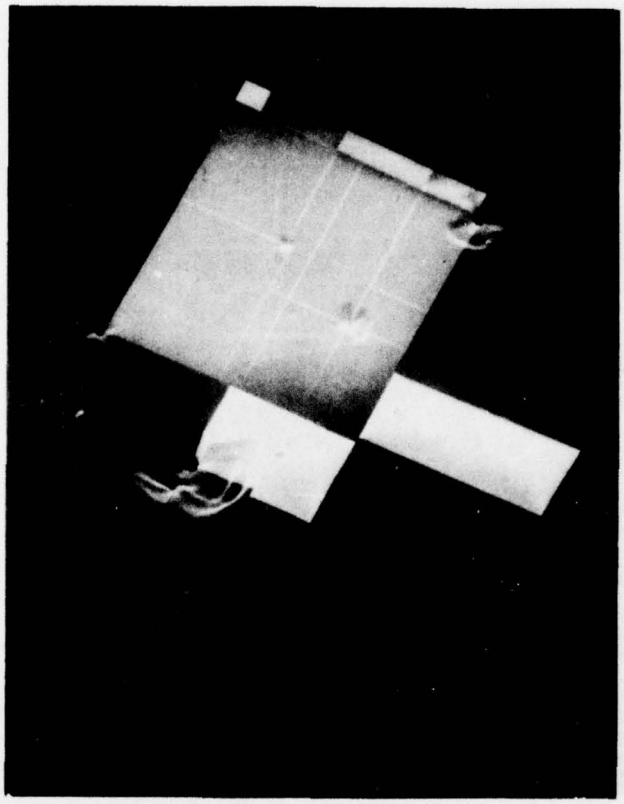

Figure IV-7. Scanning electron microscope photograph of threshold damage in a potassium chloride target. The width of the area covered by the photograph is 0.88mm.

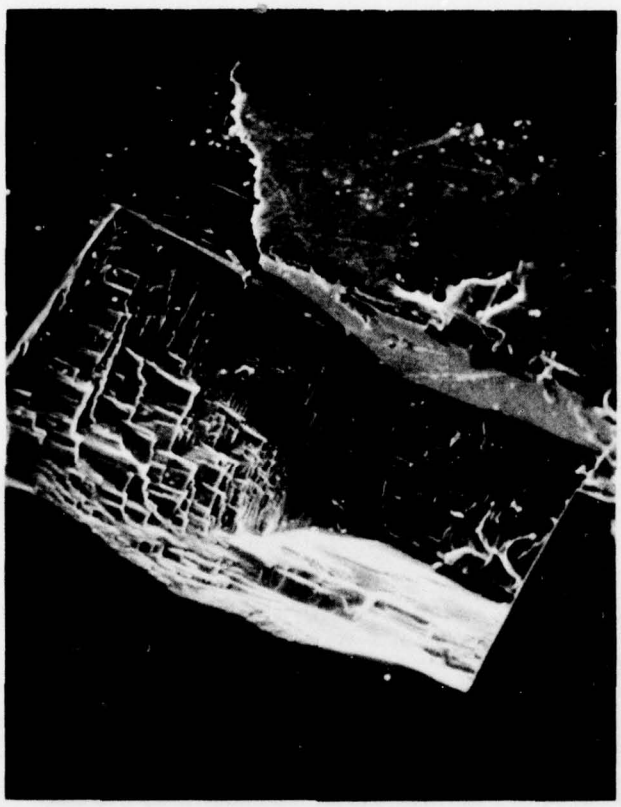

Figure IV-8. Scanning electron microscope photograph of a pit produced by impact of a TEA laser pulse at a level well above the threshold for damage on a potassium chloride surface. The width of the area covered by the photograph is 0.44mm.

before the photograph was taken. The results indicate that the damage is due to a mechanical impact resulting from the pressure pulse imparted to the sample.

The values for the observed fracture stress are somewhat low compared to theory. If one calculates a fracture stress P_f from the equation[11]

$$P_f = (2E\gamma/\pi a)^{1/2} \qquad \text{(IV-5)}$$

where E is the elastic modulus, γ the free surface energy per unit area and a the defect size, one calculates for reasonable values of the quantities in the equation[12], a fracture stress between 100 and 200 bars. On the other hand, the measured peak shock pressure near the fracture threshold is only a few bars. If one infers that the peak shock pressure was more nearly that of a metallic sample irradiated under the same conditions, the peak shock pressure would have been approximately 20 bars, with the difference resulting from the expenditure of the shock energy in producing fracture. Thus the importance of the mechanical shock in producing damage is clear, but the exact mechanism by which the damage is produced is not obvious.

In conclusion, we have presented data on the laser-induced pressure pulse as a function of the conditions of irradiation for microsecond and submicrosecond duration pulses from a CO_2 TEA laser. We have obtained scaling laws relevant for the pressure as a function of conditions of irradiation and we have related the observations of pressure to damage in single-crystalline potassium chloride.

SECTION V
DAMAGE TO PLASTIC MATERIALS

During the course of the contract period, it was agreed between the contract monitor and the principal investigator to devote some effort to irradiation of plastic materials. Samples were prepared by the Air Force Materials Laboratory and delivered to Honeywell. The surfaces were polished to an optical finish. The samples were in the form of squares with one inch sides and circular slugs of diameter 7/8". The materials are epoxy, plexiglas and silicone. The characteristics of the materials are presented in Table V-1. The purpose of the exposures of the plastics was to determine the effect of laser intensity, focussing and pulse repetition rate on gross damage to these materials.

The three materials were exposed to repetitive laser pulses and the characteristics of the damage when noted. Generally the silicone during irradiation emitted a large jet of yellow flame, along with heavy smoke. A region around the irradiated area was heavily blackened. The epoxy showed very little flame but emitted a dense jet of smoke. It also showed considerably blackening around the impact area, although not as much as with the silicone. The plexiglas emitted a faint, pale bluish-white flame, with relatively little smoke. There was very little discoloration around the edges of the impact area.

Because of the covering of the materials with smoke and soot, it was not possible to carry out as many experiments as desired. Because of the blackening of the materials around the impact area, the target areas had to be fairly well separated. It was possible to carry out only one or two experiments on a given sample of silicone or epoxy. Because the plexiglas showed relatively little blackening, it was possible to use impact areas spaced more closely. We were able to carry out more experiments on plexiglas than the other materials.

The experiments that were carried out were measurement of the mass removal per laser pulse and measurement of the depth of the hole produced. The experiments on mass removal were accomplished by weighing the samples on an analytical balance before and after irradiation by a series of one hundred shots. The depth of the hole was measured for a series of either one or two shots, using a profilometer (Taylor-Hobson Model Talysurf 10).

The data on mass loss is summarized in Table V-2. The table presents the mass removal per laser pulse, under varying conditions of laser power density, pulse repetition rate and focal area of the laser beam on the target surface. In order to present this data more clearly, some of it is plotted in Figures V-1, V-2 and V-3, which compare mass removal for different conditions. Figure V-1

TABLE V-1

Materials

Material	Description	Batch
Epoxy	DER 825 Dow Chemical	4/76-332-6-B
Plexiglas	MIL-P-8184, Acrylic 18-3	--
Silicone	2556 AVCO TR-76-212	8/3/76-2556

TABLE V-2

Summary of Data on Plastics

Laser Power Density (w/cm^2)	Pulse Rep Rate (pps)	Focal Area (cm^2)	Mass Removal per pulse (mg)
Silicone			
1.44×10^8	5.26	0.0375	0.116
4.24×10^8	5.26	0.0127	0.020
1.48×10^8	5.26	0.0127	0.010
4.24×10^8	1	0.0127	0.010
9.91×10^7	8	0.0296	0.060
9.91×10^7	1	0.0296	0.042
7.15×10^7	8	0.041	0.090
3.03×10^7	8	0.097	0.124
4.19×10^7	8	0.070	0.099
Epoxy			
1.44×10^8	5.26	0.0375	0.250
4.24×10^8	5.26	0.0127	0.069
1.48×10^8	5.26	0.0127	0.019
4.24×10^8	1	0.0127	0.010
9.91×10^7	8	0.0296	0.118
9.91×10^7	1	0.0296	0.083
7.15×10^7	8	0.041	0.160
3.03×10^7	8	0.097	0.208
4.19×10^7	8	0.070	0.180
Plexiglas			
1.44×10^8	5.26	0.0375	0.400
4.24×10^8	5.26	0.0127	0.049
3.1×10^8	5.26	0.0127	0.040
1.48×10^8	5.26	0.0127	0.030
4.24×10^8	low	0.0127	0.030
9.91×10^7	8	0.0296	0.154
9.91×10^7	1	0.0296	0.106
7.15×10^7	8	0.041	0.197
4.19×10^7	8	0.070	0.211
9.91×10^7	5.26	0.0296	0.150

TABLE V-2 (Continued)

Laser Power Density (w/cm^2)	Pulse Rep Rate (pps)	Focal Area (cm^2)	Mass Removal per pulse (mg)
9.91×10^7	3	0.0296	0.129
2.17×10^7	8	0.135	0.346
3.03×10^7	8	0.097	0.295

Figure V-1. Mass removal per pulse as a function of laser power density at 5.26 pulses per second with a focal area of $0.0127 cm^2$.

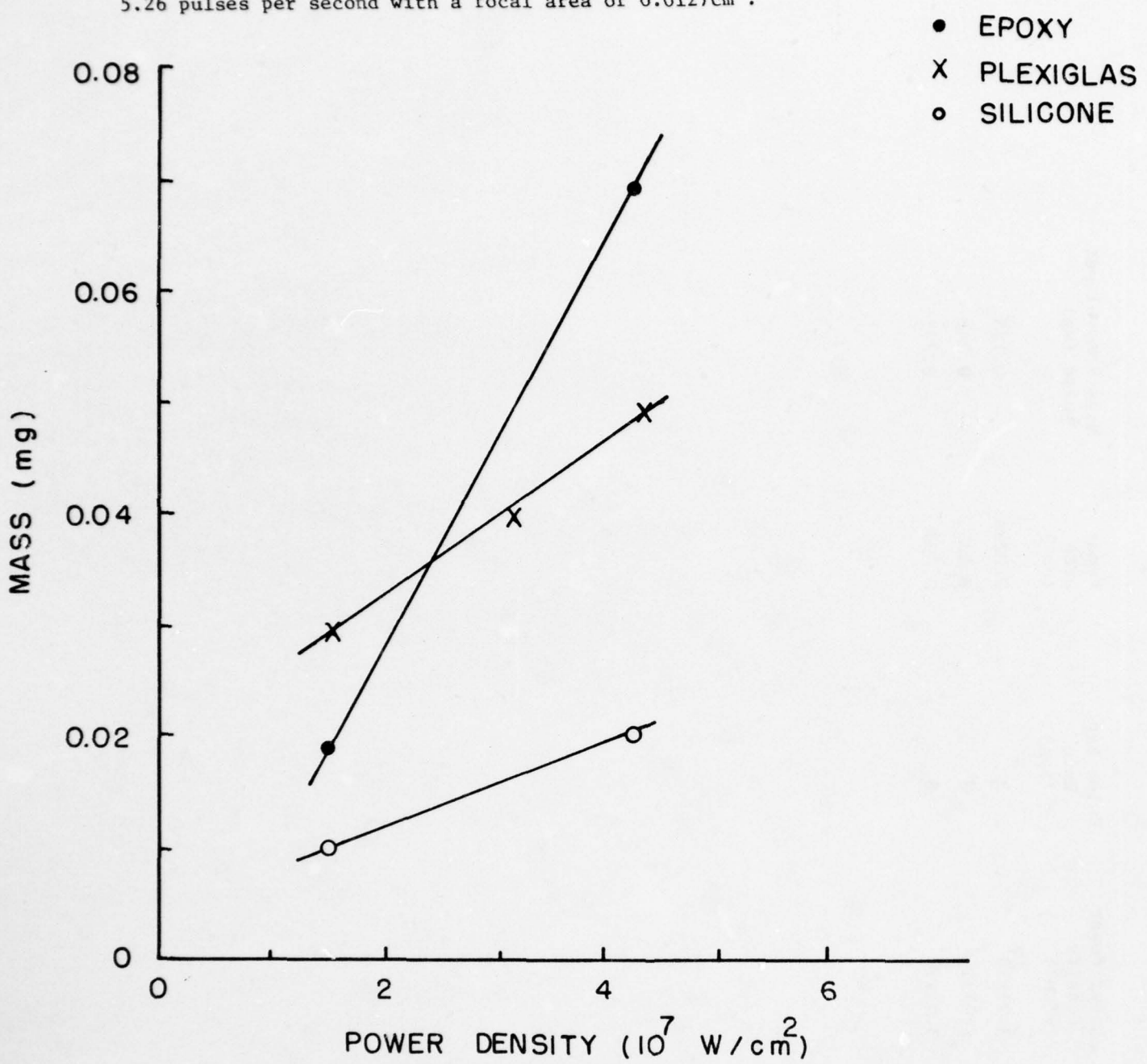

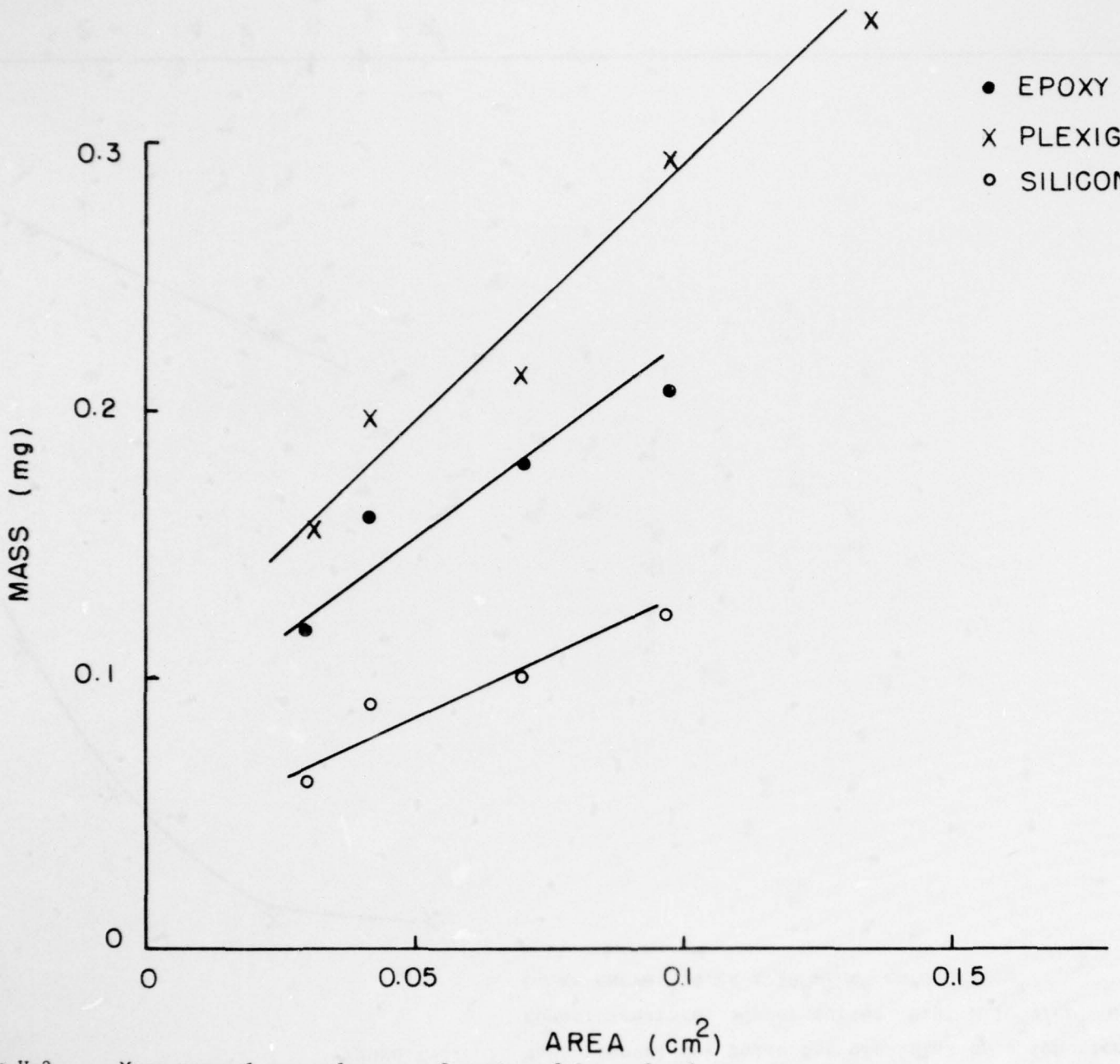

Figure V-2. Mass removal per pulse as a function of laser focal area at constant laser power and constant pulse repetition rate of 8 pulses per second.

Figure V-3. Mass removal per pulse for plexiglas as a function of pulse repetition rate. Upper curve: $9.91 \times 10^{7} w/cm^{2}$ on $0.0296 cm^{2}$. Lower curve: $4.24 \times 10^{8} w/cm^{2}$ on $0.0127 cm^{2}$.

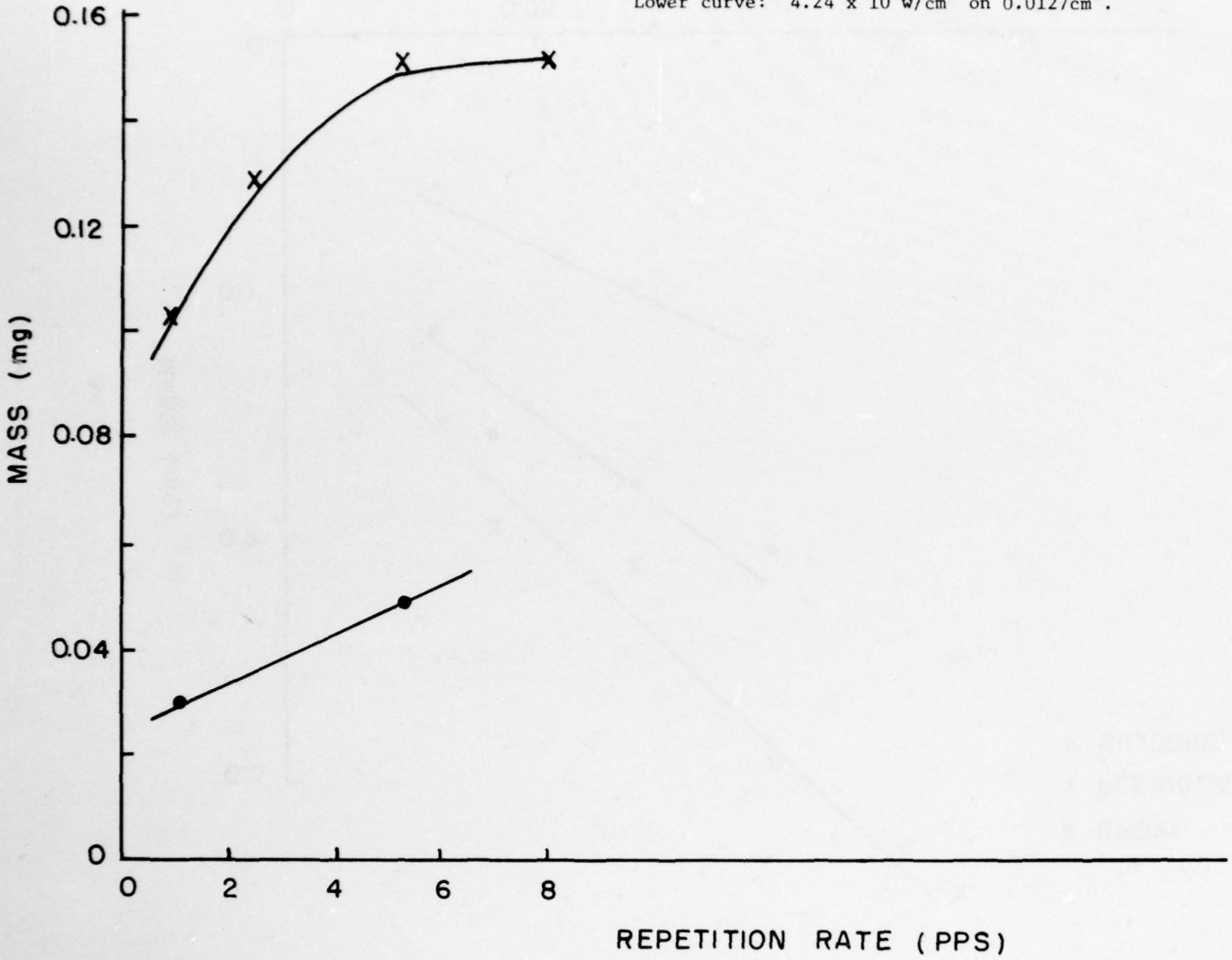

shows mass removal per pulse as a function of laser power density under conditions of constant pulse repetition rate (5.26 pulses/second) and under conditions of constant focussing (focal area 0.0127 square centimeters). The mass removal increases with increasing laser power density as expected.

The effect of changing the focal area for conditions of constant total laser power and constant pulse repetition rate are shown in Figure V-2. This result was not expected. The mass removal increases with increasing focal area, although the laser power per unit area is decreasing as the focal area is increased. This may arise because the laser-supported absorption wave will be less intense as the area is increased, under conditions of constant total power. Then the beam will be transmitted through the blowoff material and reach the surface more efficiently.

The effect of pulse repetition rate is shown in Figure V-3 for plexiglas, under two conditions of irradiation, namely $9.91 \times 10^7 w/cm^2$ incident on an area of $0.0296 cm^2$ and $4.24 \times 10^8 w/cm^2$ incident on an area of $0.0127 cm^2$. There is a increase in mass removal per pulse as the pulse repetition rate increases from one pulse per second up to about six pulses per second. There is apparently a saturation of this phenomenon after at higher pulse repetition rates. Although data are not plotted for silicone and epoxy, they too show an increase in the mass removal as the pulse repetition rate is increased from one pulse per second to the range of 5 or 8 pulses per second, with the other conditions of irradiation being unchanged. This increase is about 50%, similar to that seen with plexiglas.

This phenomenon is unexpected and we have no good explanation for it at present.

The ordering of the mass removal is of considerable interest. Under most conditions of irradiation, there is less silicone removed than epoxy or plexiglas. However, the epoxy and plexiglas have similar amounts of material removed, but the ordering depends on the exact conditions of irradiation.

The depth of the hole produced by a single pulse was measured with a profilcometer. A typical example of the hole produced in a plexiglas sample by a single pulse of laser power density $9.91 \times 10^7 w/cm^2$ incident on an area of $0.0296 cm^2$ is shown in Figure V-4. There is a considerable amount of small scale structure on the bottom of the hole. However, the excursion is confined within a total range of approximately 4 micrometers. The edges of the hole are steep and well defined. There is some indication of a raised lip around the edges of the hole.

Data on the depth of the hole as a function of laser power density are shown in Figure V-5. This shows results for material removal at an constant focus for a single shot, with the laser power being varied.

Data for volume of material removed by a single shot at constant power are shown in Figure V-6, for variable focal area. These results are in reasonably good

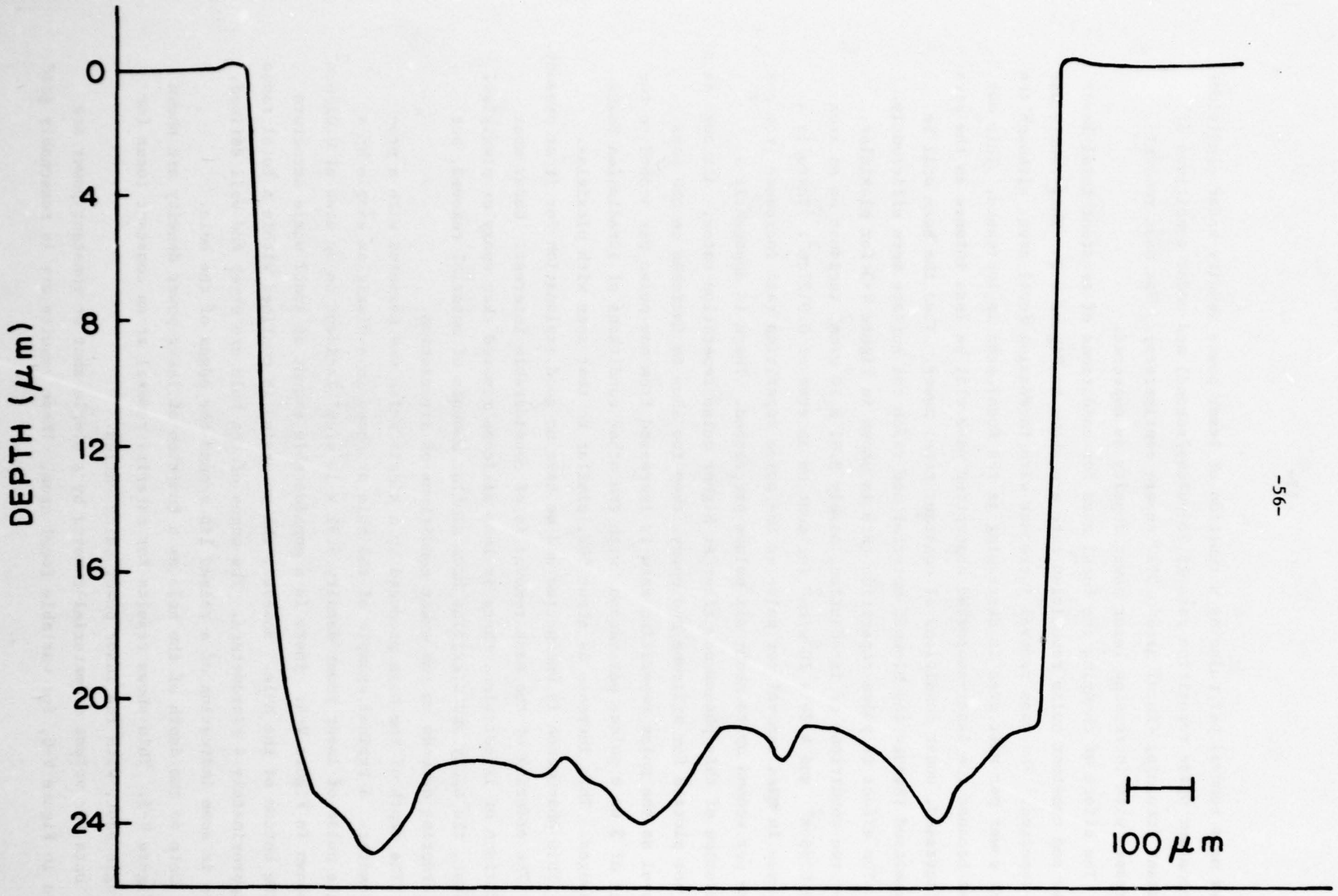

Figure V-4 Profile of a hole produced by a single pulse in a plexiglas sample with laser power density 9.91 x 10^7 w/cm^2 incident on an area of 0.0296 cm^2.

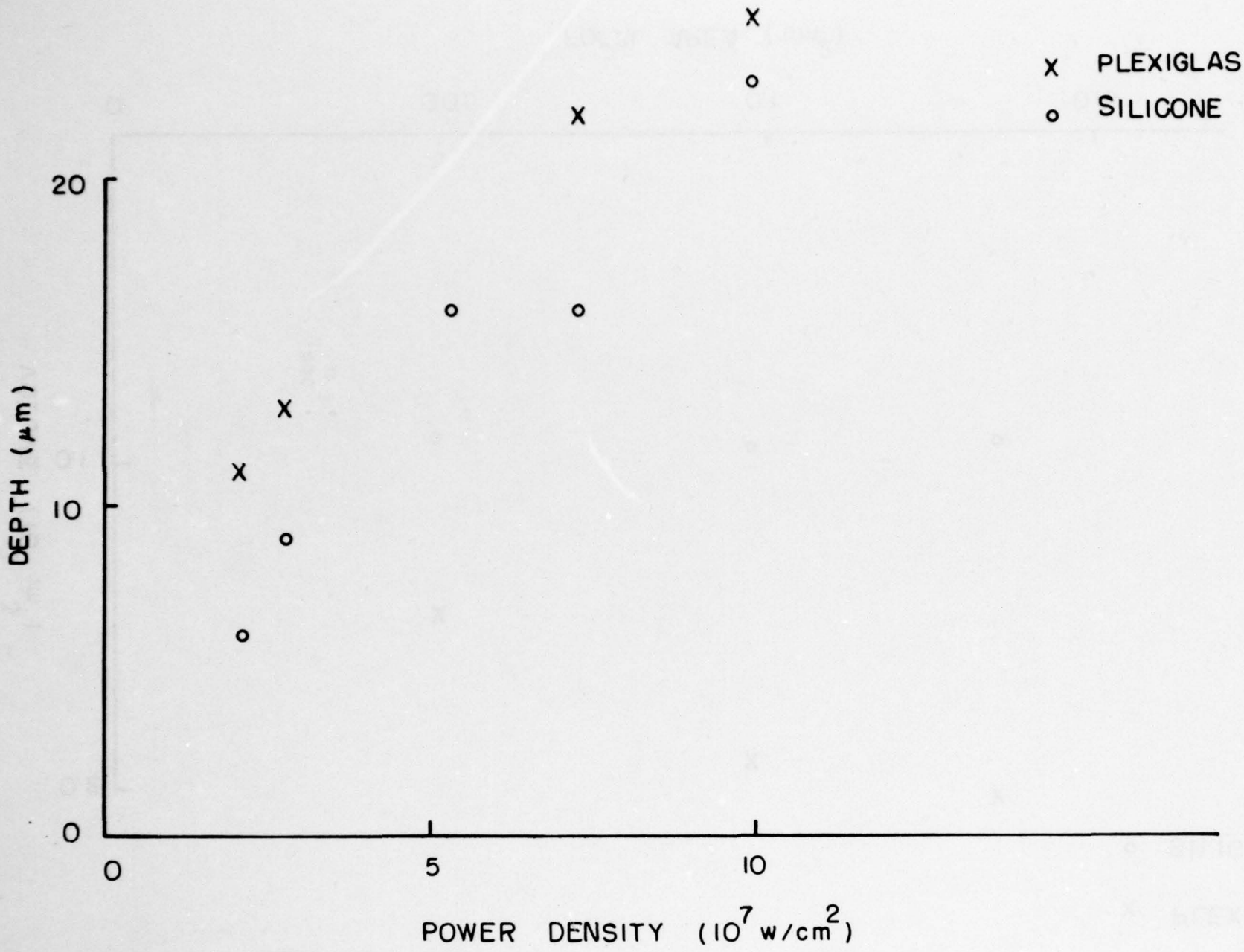

Figure V-5. Depth of hole produced as a function of laser power density at constant laser power with variable focus.

Figure V-6. Volume of material removed as a function of focal area.

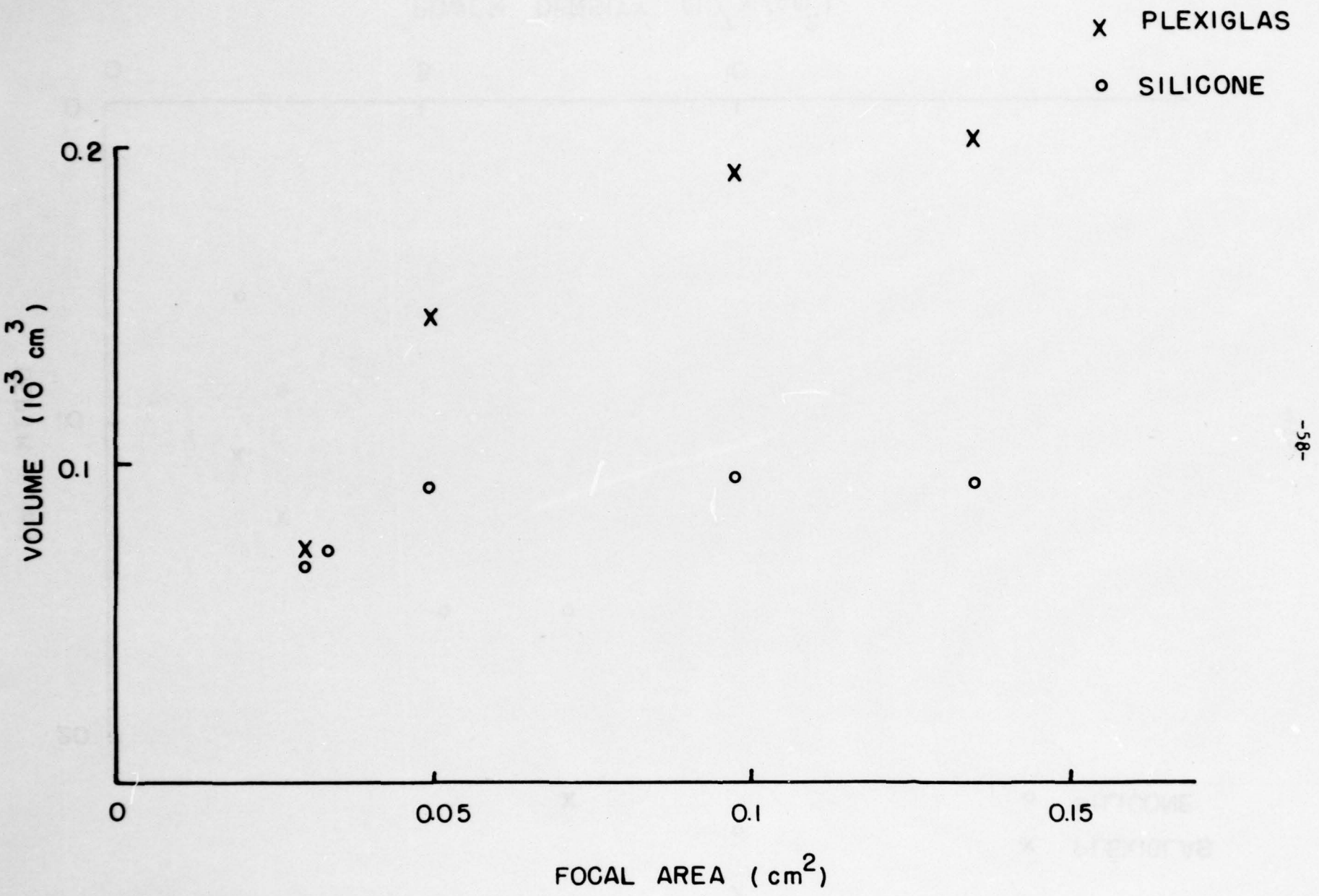

agreement with the mass removal results for a material density of $1 gm/cm^3$.

When two pulses in a row were delivered, the holes became deeper. The roughness of the bottom also increased, so that the measurements were somewhat less accurate. For plexiglas the depth of the holes approached 50 micrometers, which was the maximum depth measurable by the profileometer. Data on the hole depth produced by two successive shots are shown in Table V-3, and compared to hole depths produced by a single shot. For plexiglas, two individual shots spaced one second apart produced a hole approximately twice as deep as a single shot. Two shots spaced at a spacing of 125 milliseconds produced a slightly deeper hole, although it was not possible to determine the depth exactly because the maximum measuring capability is 50 micrometers. For silicone, the depth produced by two shots was slightly less than twice that produced by a single shot. There is also an indication that as the interpulse time decreases, the depth of the hole produced by two shots increases.

The physical phenomena involved in these results require further investigation. The variation of pulse repetition rate and focusing produce complicated changes in the damage, which are not readily explainable.

TABLE V-3

Hole Depth

($9.91 \times 10^7 w/cm^2$ pulses)

Material	Single Shot	Two Shots 1 Second Apart	Two Shots 125ms Apart
Plexiglas	25μm	50μm	$\gtrsim$50μm
Silicone	23μm	37μm	43μm

SECTION VI
SUMMARY AND CONCLUSIONS

It is appropriate to summarize the significant results obtained during this program of measurements on the properties of metallic surfaces irradiated by high power pulsed CO_2 laser radiation. We have performed a number of different types of quantitative measurements on the changes produced by interaction of CO_2 laser pulses with power density in the range above $10^8 w/cm^2$ and with pulse duration in the microsecond and submicrosecond regime. This was a region of interaction parameters which had not been thoroughly explored previous to the beginning of this work and for which understanding of the physical processes was incomplete. As a result of the work performed under this contract, and also of work performed at other laboratories, there now exists a much expanded body of quantitative data on the interaction in this regime of laser parameters.

Specifically we have obtained measurements of the following items:

- Measurements of the impulse transmitted to metallic targets by the TEA laser pulse. The impulse increases with increasing ambient air pressure as one goes from approximately 1 torr to 760 torr.

  Impulse increases from 0.4 dyne-second to the range of 5 to 10 dyne seconds. Quantitative data on the effect of changing target materials, laser pulse shape, and total laser energy are available.

- Measurements on the pressure pulse coupled into the target material. For typical conditions of laser irradiation in this regime, the peak pressure coupled into metallic targets is of the order of 100 bars, a pressure which decreases to zero within a few microseconds. The pressure pulse propagates through the target and is measured by the motion of the polished rear surface of the target. Quantitative data for the pressure as a function of ambient air pressure, laser power density and other relevant parameters have been obtained. The peak pressures are well below the values of the dynamic fracture strength of metals for laser power densities of the order of $10^8 w/cm^2$. However they do exceed the fracture strength of potassium chloride, an important window material. The observation of a pressure pulse is coupled to catastrophic cracking and pitting of the potassium chloride material.

- Measurement of the ionic species, their energies and states of ionization in the blowoff material. The ionic energies in the blowoff material are

observed to be several hundred electron volts for laser power densities of the order of $2 \times 10^8 w/cm^2$. The ion energy increases rapidly with increasing laser power density. The states of ionization in the blowoff material also increase in an orderly manner as the laser power density increases, with states of relatively low ionization (e.g. single ionization) being replaced by states of higher ionization (3 or 4 times ionized) as the laser power density increases. Also the impulse transferred to the target surface by the expanding blowoff material in its observed state of energy is approximately 0.35 dyne seconds, a value in excellent agreement with the impulse measured from the motion of the target at low ambient air pressure.

The time development of the ionic energy spectrum has been observed. At times early in the laser pulse, the ion emission occurs at relatively low values of energy. As time progresses, the peak and most probable values of the ionic energy spectrum move to higher energies. This directly indicates the effect of absorption of laser energy in the blowoff material. In addition, direct measurements of the fraction of the incident energy carried away by the blowoff material have been obtained. They are in the range of a few percent under the relevant conditions of irradiation.

- Measurement of specular reflectivity and diffuse reflectivity during and after irradiation. Time resolved data were obtained for the change in specular reflectivity during the interaction. Quantitative results are available for the change in specular reflectivity under varying conditions of irradiation, including ambient air pressure, laser power density, pulse shape and accumulated number of pulses on the same area. Measurements as a function of ambient air pressure show that the change due to a single laser shot is smaller at higher values of the ambient air pressure, indicating the effect of the laser-supported absorption wave in shielding the target surface. Results at two different probing laser wavelengths have been useful in distinguishing the mechanisms by which the surface reflectivity is changed.

Measurements of diffuse reflectivity show the transition from a specularly reflecting surface to a diffusely reflecting surface, with an accompanying increase in absorptivity near 10μm. Some results for a time-dependent absorptivity have been presented.

Let us consider briefly the physical picture to be derived from the experimental measurements. The measurements on the change of reflectivity imply that the surface

becomes damaged, through melting and vaporization of material near the top of the surface. This leads to production of a diffusely reflecting surface, with irregularities having a scale size of a few micrometers. This means that under some conditions the surface will still appear relatively smooth to 10μm radiation, but will be a very rough surface for radiation in the visible portion of the spectrum. Thus the effect of irradiation with a given set of parameters will be much enhanced when the surface is probed by a visible laser beam as compared to results when a CO_2 laser beam is used as a probe.

When the surface is damaged only moderately, as for example after a single pulse in high ambient air pressure, the specular reflectivity is degraded slightly, with the scattered radiation being contained within a small cone of solid angles surrounding the specular angle. As damage progresses, for example when a number of TEA laser shots impact the same area in succession, the diffuse scattering gradually spreads into a progressively larger cone of solid angles. On a heavily damaged surface, struck by many TEA laser pulses, the specular reflectivity drops to a very low value. The surface has become very diffuse.

The physical mechanisms appear to involve a flow of molten material on the surface. The form of the surface after the end of the pulse clearly shows the effects of splashing of molten material. The physical motion of the material presumably is due to pressure exerted by the expanding blowoff material.

This observation is also borne out by the fact that the change in reflectivity continues for a time longer than the duration of the TEA laser pulse. This would be expected if physical rearrangement of the surface material contributes to the change. In addition there is evidence that the vaporization from the surface continues after the end of the TEA laser pulse. This too would contribute to the relatively long time duration which is required for the reflectivity to approach its final value.

In modeling the physical effects, we see that the magnitude of the effect increases with increasing laser power density, increasing laser pulse duration, decreasing ambient air pressure and decreasing initial reflectivity of the target surface at 10.6μm. The results show very clearly the effect of the laser-supported detonation wave in shielding the target surface at high values of ambient air pressure.

The time-of-flight spectrometer experiments are notable for their contribution to an understanding of coupling of the laser energy into the blowoff material, which has been a significant physical issue for understanding of laser-surface interactions. First, the temporal development of the ionic energy spectra shows clearly that absorption is continuing throughout the time of the laser pulse. This

is indicated by the continuing increase in the average ion energy throughout the duration of the laser pulse. When nitrogen is on in the TEA laser, absorption of energy from the lower power microsecond-duration tail of the pulse continues to increase the average ion energy. In the case where nitrogen is off in the laser, the maximum ion energy has been reached at the end of the short laser pulse, and it does not undergo a further increase after the end of the pulse.

However, material does continue to be emitted even after the end of the short laser pulse. This is a significant result. It has implications for the coupling of laser energy into the target surface, which is an important issue in understanding of enhanced thermal coupling. It tends to support models in which the blowoff plasma in front of the surface acts as a reservoir of energy which can at least partially flow back into the surface. This can lead to continued heating of the surface, accompanied by continued plasma production, even after the laser pulse has ended.

The results have also been used to derive the total amount of energy coupled into the plasma, in conditions of low ambient air pressure. Most of the energy is deposited as thermal energy, which ultimately appears as a directed energy of expansion of the blowoff material. It is notable that even though the plasma density is relatively low, there can be measurable absorption, amounting to several percent of the incident laser energy, within the tenuous blowoff material produced in the time-of-flight spectrometer.

There is a significant interrelation between the different experimental tasks. For example, the time-of-flight spectrometer work indicating continued emission of surface material after the end of the short laser pulse influences interpretation of results of reflectivity measurements, and leads to an explanation for the time scale over which the change continues. Knowledge of the increased absorptivity near the end of the pulse also helps understand the continued ionic emission.

The time-of-flight spectrometer work also leads to an estimate for the total amount of material removed and its velocity spectrum. This leads to an estimate for momentum transfer (impulse) delivered to the target at low ambient pressures. The value of the momentum transfer deduced from these results is in excellent agreement with measurements of the impulse at low ambient air pressure. Under these conditions the dominant contribution is not the laser-supported absorption wave, but recoil of the target from the plasma produced in the interaction.

The coupling into the laser-produced blowoff material has also been used in developing a model for the transmission of pressure pulses to the target.

The results described in this report on the increase of absorptivity during the laser pulse are important for understanding the coupling of laser energy into

metallic targets, which initially have low absorptivity near 10μm. The increase in absorptivity means that a significantly greater fraction of the incident laser energy can be coupled into the metallic target. This in turn enhances the value of CO_2 lasers for applications involving metallic targets.

REFERENCES

1. Investigation of Material Damage, Interactions of TEA Laser Radiation with Surfaces, J. F. Ready, Interim Report on Contract F44620-73-C-0022, covering period from 15 December 1972 to 14 December 1973 (February 1974).

2. Investigation of Material Damage, Interactions of TEA Laser Radiation with Surfaces, J. F. Ready, Interim Report on Contract F44620-73-C-0022, covering period from 15 December 1973 to 14 December 1974 (February 1975).

3. Investigation of Material Damage, Pressure Pulses Produced by Carbon Dioxide Laser Radiation, J. F. Ready, Interim Report on Contract F44620-73-C-0022, covering period from 15 December 1974 to 14 December 1975 (February 1976).

4. Investigation of Material Damage, J. F. Ready, Interim Report on Contract F44620-73-C-0022, covering period from 15 December 1975 to 14 December 1976 (February 1977).

5. J. F. Ready, Impulse Produced by the Interaction of CO_2 TEA Laser Pulses, Appl. Phys. Lett., vol. 25, pp. 558-560, November 15, 1974.

6. J. F. Ready, Change of Reflectivity of Metallic Surfaces during Irradiation by CO_2-TEA Laser Pulses, IEEE Journal of Quantum Electronics, vol. QE-12, pp. 137-142, February 1976.

7. See, for example, R. N. Keeler and E. B. Boyce, Shock Waves in Condensed Media, in Physics of High Energy Density, Proceedings of the International School of Physics "Enrico Fermi", P. Caldirola and H. Knoepfel, eds., Academic Press, Inc., New York and London, 1971, pp. 51-150.

8. A. N. Pirri, Theory for Momentum Transfer to a Surface with a High-Power Laser, Phys. Fluids, vol. 16, pp. 1435-1440, September 1973.

9. A. N. Pirri, Theory for Laser Simulation of Hypervelocity Impact, Phys. Fluids, vol. 20, pp. 221-228, February 1977.

10. M. Bass and K. M. Leung, The Dependence of the Pulsed 10.6μm Laser Damage Threshold on the Manner in which a Sample is Irradiated , IEEE J. Quantum Electron., vol. QE-12, pp. 82-83, February 1976.

11. B. R. Lawn and T. R. Wilshaw, Fracture of Brittle Solids, Cambridge University Press, Cambridge, 1975, Chapter 1.

12. R. W. Rice, High Energy Laser Windows, Semi-Annual Report No. 1 for Period Ending 31 December 1972, Naval Research Laboratory, Washington, D.C.